A contact theory for surface tension driven systems

Roger A. Sauer [1]

Aachen Institute for Advanced Study in Computational Engineering Science (AICES), RWTH Aachen University, Templergraben 55, 52056 Aachen, Germany

Published[2] in *Mathematics and Mechanics of Solids*, DOI: 10.1177/1081286514521230
Submitted on 12. September 2013, Accepted on 5. January 2014

Abstract

This paper presents a general model description for the contact of surface tension driven systems. The example system of a liquid droplet in contact with a deformable solid substrate is considered. This can be easily modified to consider two liquids or two solids in contact. The surface kinematics, essential to the modeling of surface tension, is described here in curvilinear coordinates. In particular modeling focus are the contact conditions at the contact boundary, where a wetting ridge may develop. It is shown that in the case of quasi-statics and hyperelasticity the governing equations can be derived from a global potential that accounts for contact as well as the energy storage within the bulk and surface domains. Altogether, 21 Euler-Lagrange equation are derived in this manner. Apart from these strong form equations, the governing weak form as well as its complete linearization, which are required for computational methods, are also discussed. It is shown that the governing equations can be further simplified into a reduced set of equations that are then suitable for an efficient computational implementation of the system. Computational solution methods are not discussed here, as the present focus is on the theory and its implications. A few remarks on analytical solutions, as well as a simple computational example, are given nonetheless. An auxiliary benefit of this work is a summary of the variation and linearization of the kinematical and constitutive equations of the system.

Keywords: contact constraints, curvilinear coordinates, Euler-Lagrange equations, membrane elasticity, variational methods, wetting ridge.

1 Introduction

Surface tension driven systems can play a very important role at small length scales, where surface effects can become dominant. Since all substances – liquids, solids and gases – have surfaces at boundaries, they can all be affected by surface tension. Sometimes there is only a surface (with negligible thickness), as in the case of membranes and thin films, and consequently such systems may only be driven by surface tension. An illustrative example is a liquid droplet sitting on a soft substrate. The droplet, but also the substrate, may be governed by surface tension. Further, the surface tension will also govern the contact behavior between droplet and substrate. This setting is relevant to the wetting-, hydrophobicity- and self-cleaning-properties of solid surfaces. Examining the influence of the surface tension on solids, liquids and their contact behavior, is therefore an important issue, especially at small length scales. Here in this treatment, we are interested in assembling a very general three-dimensional model description

[1]corresponding author, email: sauer@aices.rwth-aachen.de
[2]This pdf is the personal version of an article whose final publication is available at http://mms.sagepub.com

in the context of non-linear continuum mechanics that accounts for the surface tension of two bounded bodies in contact. The problem is characterized by the coupling of five fields: the deformation of the two bodies and their three interfaces. Contact constraints are introduced to formulate the coupling. The coupled system can in general be studied by computational methods. This is not the focus here. This paper rather serves as a rigorous foundation for such computations as well as for later theoretical extensions. Furthermore, it gives an overview of the governing equations formulated in strong, weak and linearized form. It is demonstrated that for quasi-statics and hyperelasticity, these can be derived from a global potential. It is further shown how the system can be simplified, without losing essential information.

Here, the surface tension is formulated in the framework of the shell theory of Steigmann [1], disregarding the curvature elasticity inherent to shells. So we only consider an in-plane stretch-induced membrane stress state within the interfaces. Bending-induced stresses, as well as out-of-plane stresses, are not considered here, even though they may also be relevant even for fluid films [2]. The contact treatment considered here is based on the classical large-deformation approaches reported by Laursen [3] and Wriggers [4]. In the context of (the aforementioned) membranes, contact and adhesion has been studied in the work of Baesu et al. [5], Agrawal [6] and Sauer et al. [7]. In these studies, however, the specific contact conditions along the contact line are not included within the formulation, as is a focus here. Further novelties of this work are: a detailed interpretation of the stress state at the wetting ridge, the derivation of constrained membrane elasticity, the simplification into a reduced model description, and a stability discussion for constant surface tension (occurring e.g. for liquids). An auxiliary benefit is the summary of the variation and linearization of the kinematical and constitutive expressions of the studied system. To the best of our knowledge, this study seems to be the most detailed work to-date on the contact coupling of surface driven systems.

The remainder of this paper is organized as follows. Sec. 2 introduces the notation and kinematical description of the considered system. Sec. 3 then proceeds with deriving the governing Euler-Lagrange equilibrium equations based on the global potential of the system. Along the way, the variation of kinematical and constitutive expressions is discussed. The linearization of the governing equations is then presented in Sec. 4. A particular focus is placed on the reduction of the model description. Sec. 5 then presents a simple computational example for illustration. The paper concludes with Sec. 6.

2 Problem setup

This section discusses the general notation and kinematical description of the considered droplet–substrate system. A particular focus is placed on the conditions at the contact line.

2.1 Domains

Consider a liquid droplet in contact with a solid body, as shown in Fig 1. The following five domains can be identified: The droplet domain $\mathcal{D}$, the solid domain $\mathcal{B}$, the surrounding gas domain $\mathcal{G}$, which is not considered any further here, and the free surface domain

$$\mathcal{S} = \mathcal{S}_{\mathrm{LG}} \cup \mathcal{S}_{\mathrm{SL}} \cup \mathcal{S}_{\mathrm{SG}} \tag{1}$$

composed of the interfaces between liquid and gas, solid and liquid, and solid and gas. We denote the surfaces of the liquid and the solid by

$$\begin{aligned} \mathcal{S}_{\mathrm{L}} &:= \mathcal{S}_{\mathrm{LG}} \cup \mathcal{S}_{\mathrm{SL}} \ , \\ \mathcal{S}_{\mathrm{S}} &:= \mathcal{S}_{\mathrm{SL}} \cup \mathcal{S}_{\mathrm{SG}} \ . \end{aligned} \tag{2}$$

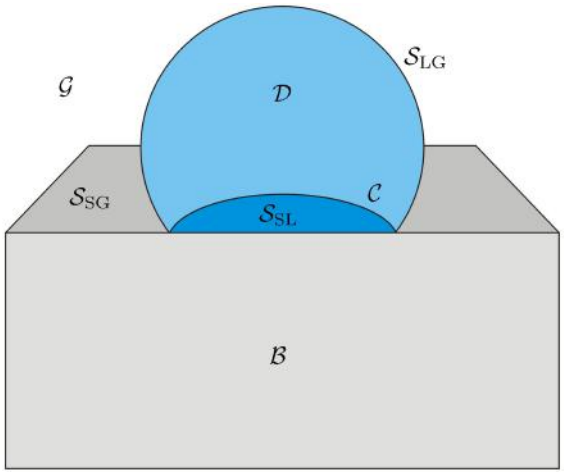

Figure 1: Problem setup: Liquid droplet $\mathcal{D}$ in contact with a deformable substrate $\mathcal{B}$.

The fifth domain to be identified here is the contact line domain

$$\mathcal{C} = \mathcal{S}_{\mathrm{LG}} \cap \mathcal{S}_{\mathrm{SL}} \cap \mathcal{S}_{\mathrm{SG}} \ , \tag{3}$$

where the three interfaces meet. The system may be viewed as closed, without boundary. In general, however, boundary conditions may be prescribed on the problem, e.g. due to symmetry conditions. If an imaginary plane, $\mathcal{P}$, cuts through the domains, the boundaries $\partial_{\mathcal{P}}\mathcal{D}$, $\partial_{\mathcal{P}}\mathcal{B}$, $\partial_{\mathcal{P}}\mathcal{S}$ and $\partial_{\mathcal{P}}\mathcal{C}$ are created. On those boundaries either displacement (Dirichlet) or traction (Neumann) boundary conditions are prescribed. Denoting the respective domains by $\partial_u\Omega$ and $\partial_t\Omega$ ($\Omega = \mathcal{B}$, $\mathcal{C}$, $\mathcal{D}$, or $\mathcal{S}$) we have

$$\partial_{\mathcal{P}}\Omega = \partial_u\Omega \cup \partial_t\Omega \ . \tag{4}$$

We also require that $\partial_u\Omega \cap \partial_t\Omega = \emptyset$, unless the prescribed displacements and tractions are perpendicular to each other. With this, the boundaries of domains $\mathcal{B}$, $\mathcal{D}$ and $\mathcal{S}$ are

$$\partial\mathcal{B} = \partial_u\mathcal{B} \cup \partial_t\mathcal{B} \cup \mathcal{S}_{\mathrm{S}} \ , \tag{5}$$

$$\partial\mathcal{D} = \partial_u\mathcal{D} \cup \partial_t\mathcal{D} \cup \mathcal{S}_{\mathrm{L}} \ , \tag{6}$$

and

$$\partial\mathcal{S}_\bullet = \partial_u\mathcal{S}_\bullet \cup \partial_t\mathcal{S}_\bullet \cup \mathcal{C} \ , \tag{7}$$

with $\bullet$ = LG, SL or SG. Further, we suppose that $\partial_{\mathcal{P}}\mathcal{B}$, $\partial_{\mathcal{P}}\mathcal{D}$ and $\partial_{\mathcal{P}}\mathcal{S}$ are defined such that $\partial_{\mathcal{P}}\mathcal{B} \cap \mathcal{S}_{\mathrm{S}} = \partial_{\mathcal{P}}\mathcal{D} \cap \mathcal{S}_{\mathrm{L}} = \partial_{\mathcal{P}}\mathcal{S} \cap \mathcal{C} = \emptyset$.

2.2 Surface kinematics

We proceed with a brief overview of the kinematical description of the interfaces. A more detailed introduction can be found for example in [7].
Surface $\mathcal{S}$ can be described by a surface parameterization $\boldsymbol{x} = \boldsymbol{x}(\xi^\alpha)$, $\alpha = 1, 2$.[3] From this we can define the co-variant tangent vectors $\boldsymbol{a}_\alpha = \partial\boldsymbol{x}/\partial\xi^\alpha$, the co-variant components of the metric tensor, $a_{\alpha\beta} = \boldsymbol{a}_\alpha \cdot \boldsymbol{a}_\beta$, the contra-variant components of the metric tensor, $[a^{\alpha\beta}] = [a_{\alpha\beta}]^{-1}$, the contra-variant tangent vectors $\boldsymbol{a}^\alpha = a^{\alpha\beta}\boldsymbol{a}_\beta$, the area change $\mathrm{d}a = J_a \,\mathrm{d}\xi^1 \,\mathrm{d}\xi^2$

[3] Here and in the following all Greek indices run from 1 to 2, and imply summation when repeated.

with $J_a = \sqrt{\det a_{\alpha\beta}}$, the surface normal $\boldsymbol{n} = \|\boldsymbol{a}_1 \times \boldsymbol{a}_2\|/J_a$, the parametric derivative of $\boldsymbol{a}_\alpha$, $\boldsymbol{a}_{\alpha,\beta} = \partial \boldsymbol{a}_\alpha / \partial \xi^\beta$, the co-variant derivative of $\boldsymbol{a}_\alpha$, $\boldsymbol{a}_{\alpha;\beta} = (\boldsymbol{n} \otimes \boldsymbol{n})\, \boldsymbol{a}_{\alpha,\beta}$, and the co-variant components of the curvature tensor $b_{\alpha\beta} = \boldsymbol{n} \cdot \boldsymbol{a}_{\alpha,\beta}$. The triads $\{\boldsymbol{a}_1, \boldsymbol{a}_2, \boldsymbol{n}\}$ and $\{\boldsymbol{a}^1, \boldsymbol{a}^2, \boldsymbol{n}\}$ form bases to describe points on $\mathcal{S}$. To characterize the deformation of $\mathcal{S}$, we introduce a reference configuration, denoted $\mathcal{S}_0$, and described by the mapping $\boldsymbol{X} = \boldsymbol{X}(\xi^\alpha)$. All the kinematical surface quantities associated with $\boldsymbol{X} \in \mathcal{S}_0$ are denoted by capital letters. From the relation between $\mathcal{S}_0$ and $\mathcal{S}$, we can define the surface deformation gradient $\boldsymbol{F} = \boldsymbol{a}_\alpha \otimes \boldsymbol{A}^\alpha$, and the area change $\mathrm{d}a = J\, \mathrm{d}A$ with $J = J_a/J_A$ and $J_A = \sqrt{\det A_{\alpha\beta}}$.

2.3 Bulk kinematics

Inside the bulk domains $\mathcal{B}$ and $\mathcal{D}$, the deformation is characterized by the usual deformation gradient $\tilde{\boldsymbol{F}} = \partial \boldsymbol{\varphi} / \partial \boldsymbol{X}$, where $\boldsymbol{x} = \boldsymbol{\varphi}(\boldsymbol{X})$ denotes the mapping of material points from reference domain ($\mathcal{B}_0$ and $\mathcal{D}_0$) to current domain ($\mathcal{B}$ and $\mathcal{D}$). The volume change between these domains is then given by $\mathrm{d}v = \tilde{J}\, \mathrm{d}V$, with $\tilde{J} = \det \tilde{\boldsymbol{F}}$. Here, a tilde is used to distinguish bulk quantities from surface quantities. Further details on the bulk kinematics can be found in the classic texts of continuum mechanics, e.g. [8].

2.4 The wetting ridge

The surface tension within the interface $\mathcal{S}_{\mathrm{LG}}$ exerts a line load onto the substrate surface $\partial\mathcal{B}$. For deformable substrates this line load leads to a ridge on $\partial\mathcal{B}$ that is known as the wetting ridge. The effect has been studied experimentally [9], theoretically – beginning with Lester [10] and ranging to the recent work of Lubarda [11] – and numerically – by finite element methods [12; 13] and molecular dynamics [14]. A review of the subject with many further references has been provided recently by Yu [15]. Usually it is either assumed that the line load is supported by a singular stress field in the substrate or that the line loads acts over a small width, associated with the 'thickness' of interface $\mathcal{S}_{\mathrm{SL}}$, which leads to a rounded cap of the otherwise sharp ridge [10; 16; 11]. However, both these viewpoints are somewhat inconsistent: stress singularities are not realistic and a phase boundary should not require a thickness. As is seen in the following section, the equations derived here allow a more detailed and consistent interpretation. This is shown in Fig. 2a: The line load γ_{LG} coming from $\mathcal{S}_{\mathrm{LG}}$ is equilibrated by the surface tensions γ_{SL} and γ_{SG} of the substrate interface. These tensions are transferred into the solid by the pressure p and the shear stress τ acting between the substrate $\mathcal{B}$ and its surface $\mathcal{S}_{\mathrm{S}}$. The shear is only present if the surface tension decreases from the peak value γ_{S} to the far-field value γ_{S}^0. Such a decrease depends on the constitutive model of the surface tension. If the surface tension of the substrate is considered constant, the shear is zero. For stiff substrates, the wetting ridge may only span a very small distance ϵ. From a macroscopic viewpoint, the substrate surface may therefore appear flat at $\mathcal{C}$ (Fig. 2b). The effect of p and τ is then perceived as a net point load $\epsilon\, \tilde{\boldsymbol{\sigma}} \boldsymbol{n}$ acting on $\partial\mathcal{B}$.[4] In order to admit this point load surface $\mathcal{S}_{\mathrm{S}}$ is regularized into

$$\mathcal{S}_{\mathrm{S}} = \mathcal{S}_{\mathrm{SL}} \cup \mathcal{S}_{\mathrm{SG}} \cup \epsilon\, \mathcal{C} \ , \tag{8}$$

as shown in Fig. 2b. Along $\mathcal{C}$, the microscopic viewpoint of Fig. 2a corresponds to Neumann's equilibrium, which is the classical viewpoint for liquid substrates. The macroscopic viewpoint of Fig. 2b corresponds to Young's equilibrium, which is the limit case for rigid solid substrates. If the substrate is a liquid or a very soft solid, one may observe Neumann's equilibrium even at the macroscale. In modeling, we can choose to capture either Neumann's view or Young's view. In

[4] Here, $\tilde{\boldsymbol{\sigma}}$ is the stress tensor of body $\mathcal{B}$; $\boldsymbol{n}$ its surface normal.

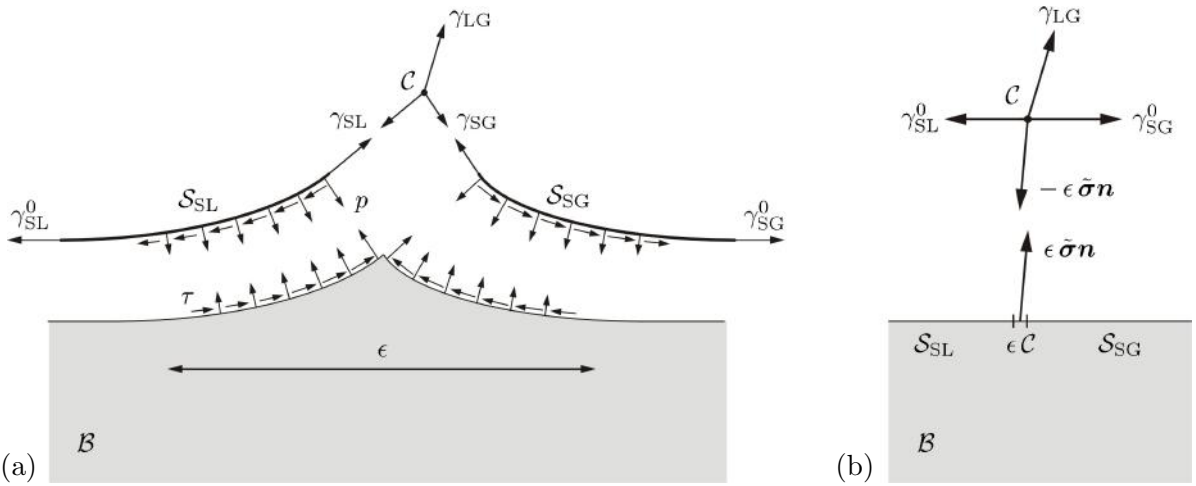

Figure 2: Conditions at $\mathcal{C}$: (a) wetting ridge (microscale view); (b) line load perceived as a stress singularity (macroscale view for $\epsilon \to 0$).

the latter case, the line load $\epsilon\,\tilde{\boldsymbol{\sigma}}\boldsymbol{n}$ appears in the model and leads to a stress singularity (unless it is regularized by the width ϵ). According to the viewpoint in Fig. 2a, no stress singularity appears in the substrate.

2.5 Restrictions

In this treatment, we restrict ourselves to quasi-static conditions, such that the liquid within $\mathcal{D}$ in governed by hydrostatic pressure that is associated with volume change $\tilde{J}$. Further, we only consider hyperelastic material behavior of the media within domains $\mathcal{B}$, $\mathcal{D}$ and $\mathcal{S}$.

3 Derivation of the governing equations

This section presents the governing equations of the droplet system introduced above. For the considered system, these follow from a global potential. The variation of that potential is discussed, leading to the weak form and the Euler-Lagrange equations governing the system. It is then shown that the system can be simplified in its complexity, leading to a reduced set of equations.

3.1 The global potential

External work that is applied to the system is considered to be stored as internal energy within the bulk domains $\mathcal{B}$ and $\mathcal{D}$, and the surface domain $\mathcal{S}$, and possibly also as contact energy within the contact interface, defined by $\mathcal{S}_{\mathrm{SL}}$ and $\mathcal{C}$.[5] We therefore consider a global potential of the form

$$\Pi = \Pi_{\mathrm{int}\mathcal{B}} + \Pi_{\mathrm{int}\mathcal{D}} + \Pi_{\mathrm{int}\mathcal{S}} + \Pi_{\mathrm{c}} - \Pi_{\mathrm{ext}} \ . \tag{9}$$

The energy stored within $\mathcal{B}$ is given by

$$\Pi_{\mathrm{int}\mathcal{B}} = \int_{\mathcal{B}_0} W_{\mathcal{B}}\,\mathrm{d}V \ , \tag{10}$$

[5]Here, we do not consider the storage of internal energy within the contact line $\mathcal{C}$, as is done in [17].

where $W_{\mathcal{B}} = W_{\mathcal{B}}(\tilde{\boldsymbol{F}})$ is the hyperelastic energy density function characterizing the solid. For a compressible fluid, the energy stored within domain $\mathcal{D}$ is given by

$$\Pi_{\mathrm{int}\mathcal{D}} = \int_{\mathcal{D}_0} W_{\mathcal{D}} \, \mathrm{d}V \ , \tag{11}$$

where $W_{\mathcal{D}} = W_{\mathcal{D}}(\tilde{J})$ is the energy density function characterizing the compressible fluid. For an incompressible fluid, $\Pi_{\mathrm{int}\mathcal{D}}$ is given by

$$\Pi_{\mathrm{int}\mathcal{D}} = \int_{\mathcal{D}_0} p_{\mathrm{f}} \, g_{\mathrm{v}} \, \mathrm{d}V \ , \tag{12}$$

where

$$g_{\mathrm{v}} = 1 - \tilde{J} = 0 \ , \tag{13}$$

defines the incompressibility constraint. The quantity p_{f} is then the associated Lagrange multiplier that physically corresponds to the fluid pressure. The energy stored within $\mathcal{S}$ is defined by

$$\Pi_{\mathrm{int}\mathcal{S}} = \int_{\mathcal{S}_0} W_{\mathcal{S}} \, \mathrm{d}A \ , \tag{14}$$

where the surface energy density is considered in the form $W_{\mathcal{S}} = W_{\mathcal{S}}(a_{\alpha\beta})$. Examples for $W_{\mathcal{S}}$ are given in Sec. 3.4 below. In general, $W_{\mathcal{S}}$ may also depend on the surface curvature and not only on the surface stretch [1].

Π_{c} denotes the contact potential. Here we consider both normal and tangential contact constraints that may act independently on the contact surface $\mathcal{S}_{\mathrm{c}} = \mathcal{S}_{\mathrm{SL}}$ and the contact line $\mathcal{C}$. This is written as

$$\Pi_{\mathrm{c}} = -\int_{\mathcal{S}_{\mathrm{c}}} p_{\mathrm{c}} \, g_{\mathrm{n}} \, \mathrm{d}a - \int_{\mathcal{S}_{\mathrm{c}}} \tau_\alpha \, g_{\mathrm{t}}^\alpha \, \mathrm{d}a - \int_{\mathcal{C}} q \, g_{\mathrm{n}} \, \mathrm{d}s - \int_{\mathcal{C}} q_\alpha \, g_{\mathrm{t}}^\alpha \, \mathrm{d}s \ , \tag{15}$$

where p_{c} and q are the Lagrange multipliers associated with the impenetrability constraint

$$g_{\mathrm{n}} = (\boldsymbol{x} - \boldsymbol{x}_{\mathrm{p}}) \cdot \boldsymbol{n}_{\mathrm{p}} \geq 0 \ , \tag{16}$$

and τ_α and q_α are the Lagrange multipliers associated with the two sticking constraints

$$g_{\mathrm{t}}^\alpha = \xi_{\mathrm{p}}^\alpha - \xi_{\mathrm{p}\,0}^\alpha = 0 \ , \quad \alpha = 1, 2 \, . \tag{17}$$

These contact constraints are defined through the closest projection of points between the neighboring bodies. Following a standard contact treatment [3; 4], we (arbitrarily) designate body $\mathcal{B}$ as master and $\mathcal{D}$ as slave body. Then, $\boldsymbol{x}_{\mathrm{p}} \in \partial\mathcal{B}$ denotes the closest projection point of some $\boldsymbol{x} \in \partial\mathcal{D}$, $\boldsymbol{n}_{\mathrm{p}}$ denotes the surface normal of $\partial\mathcal{B}$ at $\boldsymbol{x}_{\mathrm{p}}$, ξ_{p}^α denotes the parametric surface coordinate of $\boldsymbol{x}_{\mathrm{p}}$, and $\xi_{\mathrm{p}\,0}^\alpha$ denotes the initial parametric coordinate when contact first occurs. These coordinates are the solution of the two nonlinear equations

$$f_\alpha := (\boldsymbol{x} - \boldsymbol{x}_{\mathrm{p}}) \cdot \boldsymbol{a}_\alpha^{\mathrm{p}} = 0 \ . \tag{18}$$

Physically, p_{c} and τ_α correspond to surface pressure and shear, while q and q_α correspond to normal and tangential line forces. For classical solid contact, the line integrals are absent ($q = q_\alpha = 0$), while for a static droplet there is no surface friction ($\tau_\alpha = 0$). In the latter case, the line integrals are essential for capturing the tangential contact forces.

The external potential is considered in the form

$$\Pi_{\mathrm{ext}} = \int_{\mathcal{B}_0 \cup \mathcal{D}_0} \boldsymbol{x} \cdot \rho_0 \, \bar{\boldsymbol{b}} \, \mathrm{d}V + \int_{\mathcal{S} \cup \partial_t\mathcal{B}} \boldsymbol{x} \cdot \bar{\boldsymbol{f}} \, \mathrm{d}a + \int_{\partial_t\mathcal{D}} \boldsymbol{x} \cdot \bar{p} \, \boldsymbol{n} \, \mathrm{d}a + \int_{\partial_t\mathcal{S}} \boldsymbol{x} \cdot \bar{\boldsymbol{t}} \, \mathrm{d}s \ , \tag{19}$$

where $\bar{\boldsymbol{b}}$ is a prescribed, constant body force, $\bar{\boldsymbol{f}}$ is a prescribed surface traction such that $J\bar{\boldsymbol{f}}$ is constant, $\bar{p}$ is a prescribed surface pressure and $\bar{\boldsymbol{t}}$ is a prescribed line force. It is assumed that $\bar{p}\,\boldsymbol{n}\,\mathrm{d}a$ and $\bar{\boldsymbol{t}}\,\mathrm{d}s$ are invariant under deformation.
We now consider a variation of the mapping $\boldsymbol{X} \to \boldsymbol{x}$, denoted by $\delta\boldsymbol{x}$. The variation of the external potential thus is

$$\delta\Pi_{\mathrm{ext}} = \int_{\mathcal{B}_0 \cup \mathcal{D}_0} \delta\boldsymbol{x} \cdot \rho_0\, \bar{\boldsymbol{b}}\, \mathrm{d}V + \int_{\mathcal{S} \cup \partial_t\mathcal{B}} \delta\boldsymbol{x} \cdot \bar{\boldsymbol{f}}\, \mathrm{d}a + \int_{\partial_t\mathcal{D}} \delta\boldsymbol{x} \cdot \bar{p}\,\boldsymbol{n}\, \mathrm{d}a + \int_{\partial_t\mathcal{S}} \delta\boldsymbol{x} \cdot \bar{\boldsymbol{t}}\, \mathrm{d}s \ . \tag{20}$$

3.2 Variation of various kinematical quantities

The following section discusses the variation of important kinematical quantities that are later needed for the variation and linearization of Π.
The variation of $\tilde{J} = \det \tilde{\boldsymbol{F}}$ is given as

$$\delta\tilde{J} = \tilde{J}\, \mathrm{div}\, \delta\boldsymbol{x} \ , \tag{21}$$

since $\delta\tilde{J} = \partial\tilde{J}/\partial\tilde{\boldsymbol{F}} : \delta\tilde{\boldsymbol{F}}$, $\partial\tilde{J}/\partial\tilde{\boldsymbol{F}} = \tilde{J}\tilde{\boldsymbol{F}}^{-T}$ [8] and $\delta\tilde{\boldsymbol{F}} = \mathrm{grad}\,(\delta\boldsymbol{x})\,\tilde{\boldsymbol{F}}$.
The variation of the tangent vector simply is

$$\delta\boldsymbol{a}_\alpha = \delta\boldsymbol{x}_{,\alpha} \ . \tag{22}$$

Since $\delta\boldsymbol{x} = \delta x_\alpha\, \boldsymbol{a}^\alpha + \delta x\, \boldsymbol{n}$ we can expand the last result into

$$\delta\boldsymbol{x}_{,\beta} = \delta\boldsymbol{x}_{;\beta} = \delta x_{\alpha;\beta}\, \boldsymbol{a}^\alpha + \delta x_\alpha\, \boldsymbol{a}^\alpha_{;\beta} + \delta x_{;\beta}\, \boldsymbol{n} + \delta x\, \boldsymbol{n}_{;\beta} \ . \tag{23}$$

The semicolon denotes the covariant derivative w.r.t. ξ^α, which is equal to the partial derivative w.r.t. ξ^α for general vectors. According to the formula of Weingarten $\boldsymbol{n}_{;\alpha} = -b_{\alpha\beta}\, \boldsymbol{a}^\beta$.
The variation of the metric tensor is

$$\delta a_{\alpha\beta} = \boldsymbol{a}_\alpha \cdot \delta\boldsymbol{a}_\beta + \delta\boldsymbol{a}_\alpha \cdot \boldsymbol{a}_\beta \ , \tag{24}$$

which, due to (23), can also be written as

$$\delta a_{\alpha\beta} = \delta x_{\alpha;\beta} + \delta x_{\beta;\alpha} - 2\,\delta x\, b_{\alpha\beta} \ . \tag{25}$$

Here we have used $\boldsymbol{a}^\alpha_{;\beta} \cdot \boldsymbol{a}_\gamma = 0$. From $J = J_a/J_A$, $J_a = \sqrt{\det[a_{\alpha\beta}]}$, $\partial J_a/\partial a_{\alpha\beta} = \det[a_{\alpha\beta}]\, a^{\alpha\beta}$ follows first

$$\frac{\partial J}{\partial a_{\alpha\beta}} = \frac{J}{2} a^{\alpha\beta} \ , \tag{26}$$

and then with Eq. (24)

$$\delta J = \frac{J}{2} a^{\alpha\beta} \delta a_{\alpha\beta} = J\boldsymbol{a}^\alpha \cdot \delta\boldsymbol{a}_\alpha \ . \tag{27}$$

The variation of the normal vector is [4]

$$\delta\boldsymbol{n} = -\boldsymbol{a}^\alpha\, (\boldsymbol{n} \cdot \delta\boldsymbol{a}_\alpha) \ . \tag{28}$$

From $\boldsymbol{a}^\alpha \cdot \boldsymbol{a}_\beta = \delta^\alpha_\beta$ and $\boldsymbol{a}^\alpha \cdot \boldsymbol{n} = 0$ one can then obtain

$$\delta\boldsymbol{a}^\alpha = \left(a^{\alpha\beta}\, \boldsymbol{n} \otimes \boldsymbol{n} - \boldsymbol{a}^\beta \otimes \boldsymbol{a}^\alpha\right) \delta\boldsymbol{a}_\beta \ , \tag{29}$$

and evaluate the variation

$$\delta a^{\alpha\beta} = \delta\boldsymbol{a}^\alpha \cdot \boldsymbol{a}^\beta + \boldsymbol{a}^\alpha \cdot \delta\boldsymbol{a}^\beta \ . \tag{30}$$

Alternatively, $\delta a^{\alpha\beta}$ can also be computed from

$$\delta a^{\alpha\beta} = \frac{\partial a^{\alpha\beta}}{\partial a_{\gamma\delta}} \delta a_{\gamma\delta} \tag{31}$$

considering

$$a^{\alpha\beta} = \frac{1}{a} e^{\alpha\gamma}\, a_{\gamma\delta}\, e^{\delta\beta} \ , \tag{32}$$

with $a := \det a_{\alpha\beta}$ and $[e^{\alpha\beta}] = [1\ 0; -1\ 0]$. Introducing

$$m^{\alpha\beta\gamma\delta} := 2 \frac{\partial a^{\alpha\beta}}{\partial a_{\gamma\delta}} \ , \tag{33}$$

we find

$$m^{\alpha\beta\gamma\delta} = \frac{1}{a} \big(e^{\alpha\gamma} e^{\beta\delta} + e^{\alpha\delta} e^{\beta\gamma} \big) - 2 a^{\alpha\beta} a^{\gamma\delta} \ . \tag{34}$$

The variation of the line stretch $\lambda_{\mathrm{c}} := \|\boldsymbol{a}_{\mathrm{c}}\|$, where $\boldsymbol{a}_{\mathrm{c}} = \partial \boldsymbol{x}_{\mathrm{c}} / \partial \xi$ is the tangent to $\mathcal{C}$ at $\boldsymbol{x}_{\mathrm{c}}(\xi) \in \mathcal{C}$, is

$$\delta \lambda_{\mathrm{c}} = \frac{1}{\lambda_{\mathrm{c}}}\, \boldsymbol{a}_{\mathrm{c}} \cdot \delta \boldsymbol{a}_{\mathrm{c}} \ . \tag{35}$$

The variation of dependant quantities, like for example $\boldsymbol{x}_{\mathrm{p}} = \boldsymbol{x}(\boldsymbol{\xi}_{\mathrm{p}})$, is

$$\delta(\boldsymbol{x}_{\mathrm{p}}) = \delta \boldsymbol{x}(\boldsymbol{\xi}_{\mathrm{p}}) + \boldsymbol{x}_{,\alpha}(\boldsymbol{\xi}_{\mathrm{p}})\, \delta \xi^{\alpha}_{\mathrm{p}} \ . \tag{36}$$

Denoting $\delta \boldsymbol{x}_{\mathrm{p}} := \delta \boldsymbol{x}(\boldsymbol{\xi}_{\mathrm{p}})$ and $\boldsymbol{a}^{\mathrm{p}}_{\alpha} := \boldsymbol{x}_{,\alpha}(\boldsymbol{\xi}_{\mathrm{p}})$, we have in short

$$\delta(\boldsymbol{x}_{\mathrm{p}}) = \delta \boldsymbol{x}_{\mathrm{p}} + \boldsymbol{a}^{\mathrm{p}}_{\alpha}\, \delta \xi^{\alpha}_{\mathrm{p}} \ . \tag{37}$$

Analogous expressions are obtained for $\delta(\boldsymbol{a}^{\mathrm{p}}_{\alpha})$, $\delta(\boldsymbol{a}^{\alpha}_{\mathrm{p}})$ and $\delta(\boldsymbol{n}_{\mathrm{p}})$. With this, the variation of the contact constrains can be determined [3; 4]. We find

$$\delta g_{\mathrm{n}} = \big(\delta \boldsymbol{x} - \delta \boldsymbol{x}_{\mathrm{p}} - \boldsymbol{a}^{\mathrm{p}}_{\alpha}\, \delta \xi^{\alpha}_{\mathrm{p}} \big) \cdot \boldsymbol{n}_{\mathrm{p}} + (\boldsymbol{x} - \boldsymbol{x}_{\mathrm{p}}) \cdot \big(\delta \boldsymbol{n}_{\mathrm{p}} + \boldsymbol{n}_{\mathrm{p},\alpha}\, \delta \xi^{\alpha}_{\mathrm{p}} \big) \tag{38}$$

and, by taking the variation of (18),

$$\delta g^{\alpha}_{\mathrm{t}} = \delta \xi^{\alpha}_{\mathrm{p}} = c^{\alpha\beta}_{\mathrm{p}} \Big[\big(\delta \boldsymbol{x} - \delta \boldsymbol{x}_{\mathrm{p}} \big) \cdot \boldsymbol{a}^{\mathrm{p}}_{\beta} + g_{\mathrm{n}}\, \boldsymbol{n}_{\mathrm{p}} \cdot \delta \boldsymbol{x}_{\mathrm{p},\beta} \Big] \ , \tag{39}$$

where

$$\big[c^{\alpha\beta}_{\mathrm{p}} \big] := \big[a^{\mathrm{p}}_{\alpha\beta} - g_{\mathrm{n}}\, b^{\mathrm{p}}_{\alpha\beta} \big]^{-1} . \tag{40}$$

Here $\boldsymbol{a}^{\mathrm{p}}_{\beta}$, $a^{\mathrm{p}}_{\alpha\beta}$ and $b^{\mathrm{p}}_{\alpha\beta}$ are evaluated at $\boldsymbol{x}_{\mathrm{p}}$. At equilibrium, (38) simplifies to

$$\delta \hat{g}_{\mathrm{n}} = \big(\delta \boldsymbol{x} - \delta \boldsymbol{x}_{\mathrm{p}} \big) \cdot \boldsymbol{n}_{\mathrm{p}} \ , \tag{41}$$

since $\boldsymbol{a}^{\mathrm{p}}_{\alpha} \cdot \boldsymbol{n}_{\mathrm{p}} = \boldsymbol{a}^{\alpha}_{\mathrm{p}} \cdot \boldsymbol{n}_{\mathrm{p}} = 0$, while (39) simplifies to

$$\delta \hat{g}^{\alpha}_{\mathrm{t}} := \delta g^{\alpha}_{\mathrm{t}} \big|_{g_{\mathrm{n}}=0} = \big(\delta \boldsymbol{x} - \delta \boldsymbol{x}_{\mathrm{p}} \big) \cdot \boldsymbol{a}^{\alpha}_{\mathrm{p}} \ . \tag{42}$$

The hat is used to denote these special cases.

3.3 Variation of the internal potentials

This section presents the variation of the internal potentials $\Pi_{\text{int}\mathcal{B}}$, $\Pi_{\text{int}\mathcal{D}}$ and $\Pi_{\text{int}\mathcal{S}}$. The variation of Π_{c} is then discussed in Sec. 3.5.
For hyperelastic solids the first Piola-Kirchhoff stress is given by

$$\boldsymbol{P} := \frac{\partial W_{\mathcal{B}}}{\partial \tilde{\boldsymbol{F}}} \tag{43}$$

such that $\delta W_{\mathcal{B}} = \boldsymbol{P} : \delta\tilde{\boldsymbol{F}}$. Hence

$$\delta\Pi_{\text{int}\mathcal{B}} = \int_{\mathcal{B}_0} \boldsymbol{P} : \delta\tilde{\boldsymbol{F}}\, \mathrm{d}V \ , \tag{44}$$

which can also be written as

$$\delta\Pi_{\text{int}\mathcal{B}} = \int_{\mathcal{B}} \tilde{\boldsymbol{\sigma}} : \operatorname{grad}\delta\boldsymbol{x}\, \mathrm{d}v \ , \tag{45}$$

where $\tilde{\boldsymbol{\sigma}}$ is the Cauchy stress (in $\mathbb{R}^3$). With (21) and $\mathrm{d}v = \tilde{J}\,\mathrm{d}V$ we obtain for an incompressible fluid

$$\delta\Pi_{\text{int}\mathcal{D}} = -\int_{\mathcal{D}} p_{\text{f}} \operatorname{div}\delta\boldsymbol{x}\, \mathrm{d}v + \int_{\mathcal{D}_0} \delta p_{\text{f}}\, g_{\text{v}}\, \mathrm{d}V \ . \tag{46}$$

For the compressible case we have

$$\delta\Pi_{\text{int}\mathcal{D}} = -\int_{\mathcal{D}} p_{\text{f}} \operatorname{div}\delta\boldsymbol{x}\, \mathrm{d}v \ , \tag{47}$$

where the fluid pressure is now defined by

$$p_{\text{f}} := -\frac{\partial W_{\mathcal{D}}}{\partial \tilde{J}} \ . \tag{48}$$

In a similar manner to (43) and (48) we define the in-plane membrane stress $\boldsymbol{\sigma} = \sigma^{\alpha\beta}\, \boldsymbol{a}_\alpha \otimes \boldsymbol{a}_\beta$ from

$$\sigma^{\alpha\beta} := \frac{2}{J}\frac{\partial W_{\mathcal{S}}}{\partial a_{\alpha\beta}} \ . \tag{49}$$

With

$$\delta W_{\mathcal{S}} = \frac{\partial W_{\mathcal{S}}}{\partial a_{\alpha\beta}}\delta a_{\alpha\beta} \ , \tag{50}$$

(25), and $\mathrm{d}a = J\,\mathrm{d}A$ we thus have

$$\delta\Pi_{\text{int}\mathcal{S}} = \int_{\mathcal{S}} \left(\delta x_{\alpha;\beta}\, \sigma^{\alpha\beta} - \delta x\, \sigma^{\alpha\beta}\, b_{\alpha\beta}\right) \mathrm{d}a \ . \tag{51}$$

3.4 Membrane constitutive examples

To illustrate the constitutive behavior at interface $\mathcal{S}$, we present some examples. The first example is a liquid membrane with constant surface energy γ. The energy density (per reference surface) then is

$$W_{\mathcal{S}} = \gamma\, J \ , \tag{52}$$

such that $\sigma^{\alpha\beta}$ becomes

$$\sigma^{\alpha\beta} = \gamma\, a^{\alpha\beta} \ , \tag{53}$$

according to (26). Another example is

$$W_{\mathcal{S}} = \frac{\mu}{2}\Big(I_1 - 2\ln J\Big) \ , \quad I_1 := A^{\alpha\beta}\, a_{\alpha\beta} \ , \tag{54}$$

which gives

$$\sigma^{\alpha\beta} = \mu/J\big(A^{\alpha\beta} - a^{\alpha\beta}\big) \ . \tag{55}$$

This is a constitutive relation that is suitable for solids and can be used for the numerical stabilization of liquid membranes [18]. The last example considers constrained membranes. In the presence of a constraint $g = 0$, the membrane stress is given by

$$\sigma^{\alpha\beta} = \frac{2}{J}\left[\frac{\partial W_{\mathcal{S}}}{\partial a_{\alpha\beta}} + q_{\mathcal{S}}\frac{\partial g}{\partial a_{\alpha\beta}}\right] \ , \tag{56}$$

where $q_{\mathcal{S}}$ is the Lagrange multiplier associated with g. For instance, if the membrane is made of incompressible rubber, we have

$$W_{\mathcal{S}} = \mu/2\,\big(\tilde{I}_1 - 3\big) \ , \quad \tilde{I}_1 = I_1 + \lambda_3^2 \ , \tag{57}$$

and

$$g = g_{\mathrm{v}} = 1 - \tilde{J} = 0 \ , \quad (\tilde{J} = J\,\lambda_3). \tag{58}$$

Here λ_3 denotes for the out-of-plane stretch of the rubber membrane. $q_{\mathcal{S}}$ can then be obtained from the condition that the out-of-plane stress $\tilde{\sigma}_{33}$ vanishes. This stress can be found from

$$\tilde{\sigma}_{33} = \frac{1}{JT}\left[\frac{\partial W_{\mathcal{S}}}{\partial \lambda_3} + q_{\mathcal{S}}\frac{\partial g}{\partial \lambda_3}\right] \ , \tag{59}$$

see Appendix A. One finds $q_{\mathcal{S}} = \mu/J^2$ and thus

$$\sigma^{\alpha\beta} = \mu/J\big(A^{\alpha\beta} - a^{\alpha\beta}/J^2\big) \ . \tag{60}$$

This material model has been used in the computational examples of [7].

3.5 Variation of the contact potential

We now turn towards the contact potential Π_{c}. Its variation readily follows as

$$\begin{aligned}
\delta\Pi_{\mathrm{c}} = &- \int_{\mathcal{S}_{\mathrm{c}}} \Big(p_{\mathrm{c}}\,\delta g_{\mathrm{n}} + \tau_\alpha\,\delta g_{\mathrm{t}}^\alpha\Big)\,\mathrm{d}a \ - \int_{\mathcal{C}} \Big(q\,\delta g_{\mathrm{n}} + q_\alpha\,\delta g_{\mathrm{t}}^\alpha\Big)\,\mathrm{d}s \\
&- \int_{\mathcal{S}_{\mathrm{c}}} \Big(p_{\mathrm{c}}\,g_{\mathrm{n}} + \tau_\alpha\,g_{\mathrm{t}}^\alpha\Big)\,\frac{\delta J}{J}\,\mathrm{d}a \ - \int_{\mathcal{C}} \Big(q\,g_{\mathrm{n}} + q_\alpha\,g_{\mathrm{t}}^\alpha\Big)\,\frac{\delta\lambda_{\mathrm{c}}}{\lambda_{\mathrm{c}}}\,\mathrm{d}s \\
&- \int_{\mathcal{S}_{\mathrm{c}}} \Big(\delta p_{\mathrm{c}}\,g_{\mathrm{n}} + \delta\tau_\alpha\,g_{\mathrm{t}}^\alpha\Big)\,\mathrm{d}a \ - \int_{\mathcal{C}} \Big(\delta q\,g_{\mathrm{n}} + \delta q_\alpha\,g_{\mathrm{t}}^\alpha\Big)\,\mathrm{d}s \ ,
\end{aligned} \tag{61}$$

where we have used $\mathrm{d}a = J\,\mathrm{d}A$ and $\mathrm{d}s = \lambda_{\mathrm{c}}\,\mathrm{d}S$. The variation of the contact constraints is given in (38) and (39). Note, that when body $\mathcal{B}$ is rigid, we have $\delta\boldsymbol{x}_{\mathrm{p}} = \boldsymbol{0}$, such that (61) simplifies significantly. At equilibrium, where $g_{\mathrm{n}} = 0$ and $g_{\mathrm{t}}^\alpha = 0$, Eq. (61) reduces to

$$\begin{aligned}
\delta\hat{\Pi}_{\mathrm{c}} = &- \int_{\mathcal{S}_{\mathrm{c}}} \Big(p_{\mathrm{c}}\,\delta\hat{g}_{\mathrm{n}} + \tau_\alpha\,\delta\hat{g}_{\mathrm{t}}^\alpha\Big)\,\mathrm{d}a \ - \int_{\mathcal{C}} \Big(q\,\delta\hat{g}_{\mathrm{n}} + q_\alpha\,\delta\hat{g}_{\mathrm{t}}^\alpha\Big)\,\mathrm{d}s \\
&- \int_{\mathcal{S}_{\mathrm{c}}} \Big(\delta p_{\mathrm{c}}\,g_{\mathrm{n}} + \delta\tau_\alpha\,g_{\mathrm{t}}^\alpha\Big)\,\mathrm{d}a \ - \int_{\mathcal{C}} \Big(\delta q\,g_{\mathrm{n}} + \delta q_\alpha\,g_{\mathrm{t}}^\alpha\Big)\,\mathrm{d}s \ .
\end{aligned} \tag{62}$$

Inserting (41) and (42), the first line expands into

$$\begin{aligned}\delta_{\boldsymbol{x}}\hat{\Pi}_{\mathrm{c}} = &- \int_{\mathcal{S}_{\mathrm{c}}} p_{\mathrm{c}}\, \boldsymbol{n}_{\mathrm{p}} \cdot \delta\boldsymbol{x}\, \mathrm{d}a \;- \int_{\mathcal{S}_{\mathrm{c}}} \tau_\alpha\, \boldsymbol{a}_{\mathrm{p}}^\alpha \cdot \delta\boldsymbol{x}\, \mathrm{d}a \;- \int_{\mathcal{C}} q\, \boldsymbol{n}_{\mathrm{p}} \cdot \delta\boldsymbol{x}\, \mathrm{d}s \;- \int_{\mathcal{C}} q_\alpha\, \boldsymbol{a}_{\mathrm{p}}^\alpha \cdot \delta\boldsymbol{x}\, \mathrm{d}s \\ &+ \int_{\mathcal{S}_{\mathrm{c}}} p_{\mathrm{c}}\, \boldsymbol{n}_{\mathrm{p}} \cdot \delta\boldsymbol{x}_{\mathrm{p}}\, \mathrm{d}a + \int_{\mathcal{S}_{\mathrm{c}}} \tau_\alpha\, \boldsymbol{a}_{\mathrm{p}}^\alpha \cdot \delta\boldsymbol{x}_{\mathrm{p}}\, \mathrm{d}a + \int_{\mathcal{C}} q\, \boldsymbol{n}_{\mathrm{p}} \cdot \delta\boldsymbol{x}_{\mathrm{p}}\, \mathrm{d}s + \int_{\mathcal{C}} q_\alpha\, \boldsymbol{a}_{\mathrm{p}}^\alpha \cdot \delta\boldsymbol{x}_{\mathrm{p}}\, \mathrm{d}s\ .\end{aligned} \tag{63}$$

Introducing the contact traction

$$\boldsymbol{f}_{\mathrm{c}} = \tau_\alpha\, \boldsymbol{a}_{\mathrm{p}}^\alpha + p_{\mathrm{c}}\, \boldsymbol{n}_{\mathrm{p}} \quad \text{on } \mathcal{S}_{\mathrm{c}} \tag{64}$$

and contact line force

$$\boldsymbol{q}_{\mathrm{c}} = q_\alpha\, \boldsymbol{a}_{\mathrm{p}}^\alpha + q\, \boldsymbol{n}_{\mathrm{p}} \quad \text{on } \mathcal{C} \tag{65}$$

we get

$$\begin{aligned}\delta\hat{\Pi}_{\mathrm{c}} = &- \int_{\mathcal{S}_{\mathrm{c}}} \boldsymbol{f}_{\mathrm{c}} \cdot \left(\delta\boldsymbol{x} - \delta\boldsymbol{x}_{\mathrm{p}}\right) \mathrm{d}a \;- \int_{\mathcal{S}_{\mathrm{c}}} \left(\delta p_{\mathrm{c}}\, g_{\mathrm{n}} + \delta\tau_\alpha\, g_{\mathrm{t}}^\alpha\right) \mathrm{d}a \\ &- \int_{\mathcal{C}} \boldsymbol{q}_{\mathrm{c}} \cdot \left(\delta\boldsymbol{x} - \delta\boldsymbol{x}_{\mathrm{p}}\right) \mathrm{d}s \;- \int_{\mathcal{C}} \left(\delta q\, g_{\mathrm{n}} + \delta q_\alpha\, g_{\mathrm{t}}^\alpha\right) \mathrm{d}s\ .\end{aligned} \tag{66}$$

$\delta\hat{\Pi}_{\mathrm{c}}$ is an approximation to $\delta\Pi_{\mathrm{c}}$ that is exact at equilibrium. Therefore, $\delta\hat{\Pi}_{\mathrm{c}}$ may be used instead of $\delta\Pi_{\mathrm{c}}$ to determine equilibrium, even though this introduces a variational inconsistency.

3.6 Divergence Theorems

Some of the terms appearing in variations $\delta\Pi_{\mathrm{int}\mathcal{B}}$, $\delta\Pi_{\mathrm{int}\mathcal{D}}$ and $\delta\Pi_{\mathrm{int}\mathcal{S}}$ can be rewritten using the divergence theorem. This gives

$$\int_{\mathcal{B}} \tilde{\boldsymbol{\sigma}} : \operatorname{grad} \delta\boldsymbol{x}\, \mathrm{d}v = \int_{\partial\mathcal{B}} \delta\boldsymbol{x} \cdot \tilde{\boldsymbol{\sigma}}\boldsymbol{n}\, \mathrm{d}a - \int_{\mathcal{B}} \delta\boldsymbol{x} \cdot \operatorname{div} \tilde{\boldsymbol{\sigma}}\, \mathrm{d}v\ , \tag{67}$$

$$\int_{\mathcal{D}} p_{\mathrm{f}} \operatorname{div} \delta\boldsymbol{x}\, \mathrm{d}v = \int_{\partial\mathcal{D}} \delta\boldsymbol{x} \cdot p_{\mathrm{f}}\, \boldsymbol{n}\, \mathrm{d}a - \int_{\mathcal{D}} \delta\boldsymbol{x} \cdot \operatorname{grad} p_{\mathrm{f}}\, \mathrm{d}v\ , \tag{68}$$

and

$$\int_{\mathcal{S}_\bullet} \delta x_{\alpha;\beta}\, \sigma^{\alpha\beta}\, \mathrm{d}a = \int_{\partial\mathcal{S}_\bullet} \delta x_\alpha\, \sigma^{\alpha\beta}\, m_\beta\, \mathrm{d}s - \int_{\mathcal{S}_\bullet} \delta x_\alpha\, \sigma^{\alpha\beta}{}_{;\beta}\, \mathrm{d}a\ . \tag{69}$$

For the considered problem the boundaries of domains $\mathcal{B}$, $\mathcal{D}$ and $\mathcal{S}_\bullet$ are given by (5) – (7). The contribution $\epsilon\,\mathcal{C}$, according to (8), is needed in order to capture line loads acting on surface $\partial\mathcal{B}$ (see Fig. 2b). In this case, parameter $\epsilon \to 0$ is then a regularization parameter required for dimensional consistency. Note, that usually $\delta\boldsymbol{x} = \boldsymbol{0}$ on the Dirichlet boundaries $\partial_u\mathcal{B}$, $\partial_u\mathcal{D}$ and $\partial_u\mathcal{S}_\bullet$.

3.7 Euler-Lagrange equations

Given the developments of the preceding sections, we can now examine the Euler-Lagrange equation of the system. Therefore the variation of potential Π is set to zero for all possible variations of the deformation and Lagrange multipliers. The contact contribution associated

with p_c is only considered active if $p_\mathrm{c} > 0$. Otherwise this contribution is omitted. Setting the various variations to zero successively, yields the following six statements

$$\begin{aligned}
\delta_{\boldsymbol{x}}\Pi &= \delta_{\boldsymbol{x}}\Pi_\mathrm{int} + \delta_{\boldsymbol{x}}\Pi_\mathrm{c} - \delta_{\boldsymbol{x}}\Pi_\mathrm{ext} = 0 \quad \forall\, \delta\boldsymbol{x},\, \delta\boldsymbol{x}_\mathrm{p} \in \mathcal{W}\ , \\
\delta_{p_\mathrm{f}}\Pi &= \delta_{p_\mathrm{f}}\Pi_{\mathrm{int}\mathcal{D}} = 0 \quad \forall\, \delta p_\mathrm{f} \in \mathcal{P}_\mathrm{f}\ , \\
\delta_{p_\mathrm{c}}\Pi &= \delta_{p_\mathrm{c}}\Pi_\mathrm{c} = 0 \quad \forall\, \delta p_\mathrm{c} \in \mathcal{P}_\mathrm{c}\ , \\
\delta_{\tau_\alpha}\Pi &= \delta_{\tau_\alpha}\Pi_\mathrm{c} = 0 \quad \forall\, \delta\tau_\alpha \in \mathcal{T}_\alpha\ , \\
\delta_{q}\Pi &= \delta_{q}\Pi_\mathrm{c} = 0 \quad \forall\, \delta q \in \mathcal{Q}\ , \\
\delta_{q_\alpha}\Pi &= \delta_{q_\alpha}\Pi_\mathrm{c} = 0 \quad \forall\, \delta q_\alpha \in \mathcal{Q}_\alpha\ ,
\end{aligned} \tag{70}$$

where $\mathcal{W}$, $\mathcal{P}_\mathrm{f}$, $\mathcal{P}_\mathrm{c}$, $\mathcal{T}_\alpha$, $\mathcal{Q}$ and $\mathcal{Q}_\alpha$ are suitable function spaces. The last five statements, i.e.

$$\int_{\mathcal{D}_0} \delta p_\mathrm{f}\, g_\mathrm{v}\, \mathrm{d}V = 0 \quad \forall\, \delta p_\mathrm{f} \in \mathcal{P}_\mathrm{f}\ , \tag{71}$$

$$\int_{\mathcal{S}} \delta p_\mathrm{c}\, g_\mathrm{n}\, \mathrm{d}a = 0 \quad \forall\, \delta p_\mathrm{c} \in \mathcal{P}_\mathrm{c}\ , \tag{72}$$

$$\int_{\mathcal{S}} \delta\tau_\alpha\, g_\mathrm{t}^\alpha\, \mathrm{d}a = 0 \quad \forall\, \delta\tau_\alpha \in \mathcal{T}_\alpha\ , \tag{73}$$

$$\int_{\mathcal{C}} \delta q\, g_\mathrm{n}\, \mathrm{d}s = 0 \quad \forall\, \delta q \in \mathcal{Q}\ , \tag{74}$$

and

$$\int_{\mathcal{C}} \delta q_\alpha\, g_\mathrm{t}^\alpha\, \mathrm{d}s = 0 \quad \forall\, \delta q_\alpha \in \mathcal{Q}_\alpha\ , \tag{75}$$

give back the incompressibility constraint $g_\mathrm{v} = 0$ and the four contact constraints $g_\mathrm{n} = 0$ on $\mathcal{S}_\mathrm{c}$, $g_\mathrm{t}^\alpha = 0$ on $\mathcal{S}_\mathrm{c}$, $g_\mathrm{n} = 0$ on $\mathcal{C}$ and g_t^α on $\mathcal{C}$ that are active during contact.

The first equation, (70.1), can be split into two separate systems, composed of the droplet $\mathcal{D}$ and the substrate $\mathcal{B}$. By choice, we attribute the internal energy of interface $\mathcal{S}_\mathrm{SL}$ to the droplet system. Setting the variation $\delta\boldsymbol{x} = \boldsymbol{0}$ on each system, yields

$$\begin{aligned}
\delta_{\boldsymbol{x}_\mathcal{D}}\Pi = &\int_{\mathcal{D}} \left[-p_\mathrm{f}\, \mathrm{div}\, \delta x - \rho\, \bar{\boldsymbol{b}} \cdot \delta\boldsymbol{x} \right] \mathrm{d}v - \int_{\partial_t\mathcal{D}} \bar{p}\, \boldsymbol{n} \cdot \delta\boldsymbol{x}\, \mathrm{d}a \\
&+ \int_{\mathcal{S}_\mathrm{L}} \left[\sigma^{\alpha\beta}\, \delta x_{\alpha;\beta} - \sigma^{\alpha\beta}\, b_{\alpha\beta}\, \delta x - \bar{\boldsymbol{f}} \cdot \delta\boldsymbol{x} \right] \mathrm{d}a - \int_{\partial_t\mathcal{S}_\mathrm{L}} \bar{\boldsymbol{t}} \cdot \delta\boldsymbol{x}\, \mathrm{d}a \\
&- \int_{\mathcal{S}_\mathrm{c}} \boldsymbol{f}_\mathrm{c} \cdot \delta\boldsymbol{x}\, \mathrm{d}a - \int_{\mathcal{C}} \boldsymbol{q}_\mathrm{c} \cdot \delta\boldsymbol{x}\, \mathrm{d}s = 0\ , \quad \forall \delta\boldsymbol{x} \in \mathcal{W}_\mathcal{D}
\end{aligned} \tag{76}$$

for the droplet system, and

$$\begin{aligned}
\delta_{\boldsymbol{x}_\mathcal{B}}\Pi = &\int_{\mathcal{B}} \left[\tilde{\boldsymbol{\sigma}} : \mathrm{grad}\, \delta\boldsymbol{x} - \rho\, \bar{\boldsymbol{b}} \cdot \delta\boldsymbol{x} \right] \mathrm{d}v - \int_{\partial_t\mathcal{B}} \bar{\boldsymbol{f}} \cdot \delta\boldsymbol{x}\, \mathrm{d}a \\
&+ \int_{\mathcal{S}_\mathrm{SG}} \left[\sigma^{\alpha\beta}\, \delta x_{\alpha;\beta} - \sigma^{\alpha\beta}\, b_{\alpha\beta}\, \delta x - \bar{\boldsymbol{f}} \cdot \delta\boldsymbol{x} \right] \mathrm{d}a - \int_{\partial_t\mathcal{S}_\mathrm{SG}} \bar{\boldsymbol{t}} \cdot \delta\boldsymbol{x}\, \mathrm{d}a \\
&+ \int_{\mathcal{S}_\mathrm{c}} \boldsymbol{f}_\mathrm{c} \cdot \delta\boldsymbol{x}\, \mathrm{d}a + \int_{\mathcal{C}} \boldsymbol{q}_\mathrm{c} \cdot \delta\boldsymbol{x}\, \mathrm{d}s = 0, \quad \forall \delta\boldsymbol{x} \in \mathcal{W}_\mathcal{B}
\end{aligned} \tag{77}$$

for the substrate system. Here, $\mathcal{W}_\mathcal{D}$ and $\mathcal{W}_\mathcal{B}$ denote the kinematically admissible function spaces for the two systems, and $\delta\boldsymbol{x}_\mathrm{p}$, the variation of the surface point $\boldsymbol{x}_\mathrm{p} \in \partial\mathcal{B}$, has been replaced by the equivalent symbol $\delta\boldsymbol{x}$. As seen, the two systems are coupled by the contact forces $\boldsymbol{f}_\mathrm{c}$

and $\boldsymbol{q}_\mathrm{c}$. It is noted that these forces are defined in Sec. 3.5 at equilibrium. If the system is investigated in another configuration, the more general formulation appearing in (61) needs to be considered for the coupling. In this case a split into systems (76) and (77) is not straight forward. Eqs. (76) and (77) are the governing weak form equations of the two systems. They are the basis of a finite element discretization of the problem [18]. With the help of the divergence theorem, Eq. (76) can be rewritten into

$$\begin{aligned}
0 \;=\; & \int_{\mathcal{D}} \left(-\operatorname{grad} p_\mathrm{f} + \rho\, \bar{\boldsymbol{b}} \right) \cdot \delta\boldsymbol{x} \,\mathrm{d}v + \int_{\partial_t \mathcal{D}} \left(p_\mathrm{f} + \bar{p} \right) \boldsymbol{n} \cdot \delta\boldsymbol{x} \,\mathrm{d}a + \int_{\mathcal{S}_\mathrm{LG} \cup \mathcal{S}_\mathrm{SL}} p_\mathrm{f}\, \boldsymbol{n} \cdot \delta\boldsymbol{x} \,\mathrm{d}a \\
& + \int_{\mathcal{S}_\mathrm{LG}} \left[\sigma^{\alpha\beta}_{\mathrm{LG};\beta}\, \delta x_\alpha + \sigma^{\alpha\beta}_\mathrm{LG}\, b_{\alpha\beta}\, \delta x + \bar{\boldsymbol{f}} \cdot \delta\boldsymbol{x} \right] \mathrm{d}a + \int_{\partial_t \mathcal{S}_\mathrm{LG}} \left(\bar{t}^\alpha - t^\alpha_\mathrm{LG} \right) \delta x_\alpha \,\mathrm{d}s - \int_{\mathcal{C}} t^\alpha_\mathrm{LG}\, \delta x_\alpha \,\mathrm{d}s \\
& + \int_{\mathcal{S}_\mathrm{SL}} \left[\sigma^{\alpha\beta}_{\mathrm{SL};\beta}\, \delta x_\alpha + \sigma^{\alpha\beta}_\mathrm{SL}\, b_{\alpha\beta}\, \delta x + \bar{\boldsymbol{f}} \cdot \delta\boldsymbol{x} \right] \mathrm{d}a + \int_{\partial_t \mathcal{S}_\mathrm{SL}} \left(\bar{t}^\alpha - t^\alpha_\mathrm{SL} \right) \delta x_\alpha \,\mathrm{d}s - \int_{\mathcal{C}} t^\alpha_\mathrm{SL}\, \delta x_\alpha \,\mathrm{d}s \\
& + \int_{\mathcal{S}_\mathrm{c}} \boldsymbol{f}_\mathrm{c} \cdot \delta\boldsymbol{x} \,\mathrm{d}a + \int_{\mathcal{C}} \boldsymbol{q}_\mathrm{c} \cdot \delta\boldsymbol{x} \,\mathrm{d}s \;.
\end{aligned} \tag{78}$$

This can be further rearranged into

$$\begin{aligned}
0 \;=\; & \int_{\mathcal{D}} \left(-\operatorname{grad} p_\mathrm{f} + \rho\, \bar{\boldsymbol{b}} \right) \cdot \delta\boldsymbol{x} \,\mathrm{d}v + \int_{\partial_t \mathcal{D}} \left(p_\mathrm{f} + \bar{p} \right) \boldsymbol{n} \cdot \delta\boldsymbol{x} \,\mathrm{d}a \\
& + \int_{\mathcal{S}_\mathrm{LG}} \left[\left(\sigma^{\alpha\beta}_{\mathrm{LG};\beta} + \bar{f}^\alpha \right) \delta x_\alpha + \left(\sigma^{\alpha\beta}_\mathrm{LG}\, b_{\alpha\beta} + p_\mathrm{f} + \bar{p} \right) \delta x \right] \mathrm{d}a \\
& + \int_{\mathcal{S}_\mathrm{SL}} \left[\left(\sigma^{\alpha\beta}_{\mathrm{SL};\beta} + f^\alpha_\mathrm{c} + \bar{f}^\alpha \right) \delta x_\alpha + \left(\sigma^{\alpha\beta}_\mathrm{SL}\, b_{\alpha\beta} + p_\mathrm{f} - p_\mathrm{c} + \bar{p} \right) \delta x \right] \mathrm{d}a \\
& + \int_{\partial_t \mathcal{S}_\mathrm{LG}} \left(\bar{\boldsymbol{t}} - \boldsymbol{t}_\mathrm{LG} \right) \delta \boldsymbol{x}_\alpha \,\mathrm{d}s + \int_{\partial_t \mathcal{S}_\mathrm{SL}} \left(\bar{\boldsymbol{t}} - \boldsymbol{t}_\mathrm{SL} \right) \delta \boldsymbol{x}_\alpha \,\mathrm{d}s - \int_{\mathcal{C}} \left(\boldsymbol{q}_\mathrm{c} - \boldsymbol{t}_\mathrm{LG} - \boldsymbol{t}_\mathrm{SL} \right) \cdot \delta\boldsymbol{x} \,\mathrm{d}s \;.
\end{aligned} \tag{79}$$

Applying the divergence theorem to Eq. (77) gives

$$\begin{aligned}
0 \;=\; & \int_{\mathcal{B}} \left(\operatorname{div} \tilde{\boldsymbol{\sigma}} + \rho\, \bar{\boldsymbol{b}} \right) \cdot \delta\boldsymbol{x} \,\mathrm{d}v + \int_{\partial_t \mathcal{B}} \left(\bar{\boldsymbol{f}} - \tilde{\boldsymbol{\sigma}} \boldsymbol{n} \right) \cdot \delta\boldsymbol{x} \,\mathrm{d}a - \int_{\mathcal{S}_\mathrm{S} \cup \epsilon \mathcal{C}} \delta\boldsymbol{x} \cdot \tilde{\boldsymbol{\sigma}} \boldsymbol{n} \,\mathrm{d}a \\
& + \int_{\mathcal{S}_\mathrm{SG}} \left[\sigma^{\alpha\beta}_{\mathrm{SG};\beta}\, \delta x_\alpha + \sigma^{\alpha\beta}_\mathrm{SG}\, b_{\alpha\beta}\, \delta x + \bar{\boldsymbol{f}} \cdot \delta\boldsymbol{x} \right] \mathrm{d}a + \int_{\partial_t \mathcal{S}_\mathrm{SG}} \left(\bar{t}^\alpha - t^\alpha_\mathrm{SG} \right) \delta x_\alpha \,\mathrm{d}s - \int_{\mathcal{C}} t^\alpha_\mathrm{SG}\, \delta x_\alpha \,\mathrm{d}s \\
& - \int_{\mathcal{S}_\mathrm{c}} \boldsymbol{f}_\mathrm{c} \cdot \delta\boldsymbol{x} \,\mathrm{d}a - \int_{\mathcal{C}} \boldsymbol{q}_\mathrm{c} \cdot \delta\boldsymbol{x} \,\mathrm{d}s \;.
\end{aligned} \tag{80}$$

Denoting $\tilde{\sigma}^\alpha := \boldsymbol{a}^\alpha \cdot \tilde{\boldsymbol{\sigma}} \boldsymbol{n}$ and $\tilde{\sigma} := \boldsymbol{n} \cdot \tilde{\boldsymbol{\sigma}} \boldsymbol{n}$, this can be further rearranged into

$$\begin{aligned}
0 \;=\; & \int_{\mathcal{B}} \left(\operatorname{div} \tilde{\boldsymbol{\sigma}} + \rho\, \bar{\boldsymbol{b}} \right) \cdot \delta\boldsymbol{x} \,\mathrm{d}v + \int_{\partial_t \mathcal{B}} \left(\bar{\boldsymbol{f}} - \tilde{\boldsymbol{\sigma}} \boldsymbol{n} \right) \cdot \delta\boldsymbol{x} \,\mathrm{d}a \\
& + \int_{\mathcal{S}_\mathrm{SG}} \left[\left(\sigma^{\alpha\beta}_{\mathrm{SG};\beta} + \bar{f}^\alpha - \tilde{\sigma}^\alpha \right) \delta x_\alpha + \left(\sigma^{\alpha\beta}_\mathrm{SG}\, b_{\alpha\beta} + \bar{p} - \tilde{\sigma} \right) \delta x \right] \mathrm{d}a \\
& + \int_{\partial_t \mathcal{S}_\mathrm{SG}} \left(\bar{\boldsymbol{t}} - \boldsymbol{t}_\mathrm{SG} \right) \delta \boldsymbol{x}_\alpha \,\mathrm{d}s - \int_{\mathcal{S}_\mathrm{c}} \left(\boldsymbol{f}_\mathrm{c} + \tilde{\boldsymbol{\sigma}} \boldsymbol{n} \right) \cdot \delta\boldsymbol{x} \,\mathrm{d}a - \int_{\mathcal{C}} \left(\boldsymbol{q}_\mathrm{c} + \boldsymbol{t}_\mathrm{SG} + \epsilon\, \tilde{\boldsymbol{\sigma}} \boldsymbol{n} \right) \cdot \delta\boldsymbol{x} \,\mathrm{d}s \;.
\end{aligned} \tag{81}$$

Note, that due to

$$\boldsymbol{t}^\alpha_{;\alpha} = \sigma^{\alpha\beta}{}_{;\beta}\, \boldsymbol{a}_\alpha + \sigma^{\alpha\beta} b_{\alpha\beta}\, \boldsymbol{n} \;, \tag{82}$$

the middle part can be rewritten into

$$\int_{\mathcal{S}_\mathrm{SG}} \left(\boldsymbol{t}^\alpha_{\mathrm{SG};\alpha} + \bar{\boldsymbol{f}} - \tilde{\boldsymbol{\sigma}} \boldsymbol{n} \right) \cdot \delta\boldsymbol{x} \,\mathrm{d}a \;. \tag{83}$$

Now, by considering $\delta\boldsymbol{x} = \boldsymbol{0}$ successively on the various domains[6] we obtain the remaining Euler-Lagrange equations

$$\operatorname{grad} p_\mathrm{f} - \rho\,\bar{\boldsymbol{b}} = \boldsymbol{0} \qquad \text{on } \mathcal{D}\ , \tag{84}$$

$$-p_\mathrm{f} = \bar{p} \qquad \text{on } \partial_t\mathcal{D}\ , \tag{85}$$

$$\sigma^{\alpha\beta}_{\mathrm{LG};\beta} + \bar{f}^\alpha = 0 \qquad \text{on } \mathcal{S}_\mathrm{LG}\ , \tag{86}$$

$$\sigma^{\alpha\beta}_\mathrm{LG}\, b_{\alpha\beta} + p_\mathrm{f} + \bar{p} = 0 \qquad \text{on } \mathcal{S}_\mathrm{LG}\ , \tag{87}$$

$$\boldsymbol{t}_\mathrm{LG} = \bar{\boldsymbol{t}} \qquad \text{on } \partial_t\mathcal{S}_\mathrm{LG}\ , \tag{88}$$

$$\sigma^{\alpha\beta}_{\mathrm{SL};\beta} + f^\alpha_\mathrm{c} + \bar{f}^\alpha = 0 \qquad \text{on } \mathcal{S}_\mathrm{SL}\ , \tag{89}$$

$$\sigma^{\alpha\beta}_\mathrm{SL}\, b_{\alpha\beta} + p_\mathrm{f} - p_\mathrm{c} + \bar{p} = 0 \qquad \text{on } \mathcal{S}_\mathrm{SL}\ , \tag{90}$$

$$\boldsymbol{t}_\mathrm{SL} = \bar{\boldsymbol{t}} \qquad \text{on } \partial_t\mathcal{S}_\mathrm{SL}\ , \tag{91}$$

$$\boldsymbol{t}_\mathrm{LG} + \boldsymbol{t}_\mathrm{SL} = \boldsymbol{q}_\mathrm{c} \qquad \text{on } \mathcal{C}\ , \tag{92}$$

$$\operatorname{div}\tilde{\boldsymbol{\sigma}} + \rho\,\bar{\boldsymbol{b}} = \boldsymbol{0} \qquad \text{on } \mathcal{B}\ , \tag{93}$$

$$\tilde{\boldsymbol{\sigma}}\boldsymbol{n} = \bar{\boldsymbol{f}} \qquad \text{on } \partial_t\mathcal{B}\ , \tag{94}$$

$$\sigma^{\alpha\beta}_{\mathrm{SG};\beta} - \tilde{\sigma}^\alpha + \bar{f}^\alpha = 0 \qquad \text{on } \mathcal{S}_\mathrm{SG}\ , \tag{95}$$

$$\sigma^{\alpha\beta}_\mathrm{SG}\, b_{\alpha\beta} - \tilde{\sigma} + \bar{p} = 0 \qquad \text{on } \mathcal{S}_\mathrm{SG}\ , \tag{96}$$

$$\boldsymbol{t}_\mathrm{SG} = \bar{\boldsymbol{t}} \qquad \text{on } \partial_t\mathcal{S}_\mathrm{SG}\ , \tag{97}$$

$$\tilde{\boldsymbol{\sigma}}\boldsymbol{n} = -\boldsymbol{f}_\mathrm{c} \qquad \text{on } \mathcal{S}_\mathrm{SL}\ , \tag{98}$$

$$\boldsymbol{t}_\mathrm{SG} + \epsilon\,\tilde{\boldsymbol{\sigma}}\boldsymbol{n} = -\boldsymbol{q}_\mathrm{c} \qquad \text{on } \mathcal{C}\ . \tag{99}$$

Altogether, the considered system is thus governed by 21 Euler-Lagrange equations. It is noted, that it is straight forward to modify the presented system, such that also body $\mathcal{D}$ is governed by a general equilibrium equation of the form (93). Likewise, one can also modify the system such that $\mathcal{B}$ is governed by an equation of the form (84).

3.8 Simplification: Reduced set of governing equations

The set of Euler-Lagrange equations can be reduced and simplified by considering eliminations and analytical solutions. Considering an incompressible fluid, where $\rho = \rho_0$, Eq. (84) is solved by

$$p_\mathrm{f} = \boldsymbol{x}\cdot\rho\,\bar{\boldsymbol{b}} + p_\mathrm{v}\ , \tag{100}$$

where p_v is an unknown datum pressure at the origin that is discussed further below. We can thus eliminate p_f as well as $\boldsymbol{f}_\mathrm{c}$ and $\boldsymbol{q}_\mathrm{c}$ from the set of Euler-Lagrange equations. The remaining

[6] First consider $\delta\boldsymbol{x} = \boldsymbol{0}$ on all surfaces and lines to obtain (84) and (93). Then use these results and consider $\delta\boldsymbol{x} = \boldsymbol{0}$ on all line boundaries and on selected surfaces to obtain (85), (86), (87), (89), (90), (94), (95), (96) and (98). Finally use the previous results and $\delta\boldsymbol{x} = \boldsymbol{0}$ on selected line boundaries to obtain (88), (91), (92), (97) and (99).

equilibrium equations are thus given by Eqs. (86)–(88), Eqs. (93)–(97) and

$$\sigma^{\alpha\beta}_{\mathrm{SL};\beta} - \tilde{\sigma}^{\alpha} + \bar{f}^{\alpha} = 0 \quad \text{on } \mathcal{S}_{\mathrm{SL}} \ , \tag{101}$$

$$\sigma^{\alpha\beta}_{\mathrm{SL}}\, b_{\alpha\beta} + p_{\mathrm{f}} - \tilde{\sigma} + \bar{p} = 0 \quad \text{on } \mathcal{S}_{\mathrm{SL}} \ , \tag{102}$$

$$\boldsymbol{t}_{\mathrm{SL}} = \bar{\boldsymbol{t}} \quad \text{on } \partial_t \mathcal{S}_{\mathrm{SL}} \ , \tag{103}$$

$$\boldsymbol{t}_{\mathrm{LG}} + \boldsymbol{t}_{\mathrm{SL}} + \boldsymbol{t}_{\mathrm{SG}} + \epsilon\, \tilde{\boldsymbol{\sigma}} \boldsymbol{n} = \boldsymbol{0} \quad \text{on } \mathcal{C} \ . \tag{104}$$

According to the viewpoint in Fig. 2a, $\epsilon\, \tilde{\boldsymbol{\sigma}} \boldsymbol{n}$ is absent from the last equation, which is then Neumann's equilibrium. On the other hand, according to the viewpoint in Fig. 2b, $\epsilon\, \tilde{\boldsymbol{\sigma}} \boldsymbol{n}$ is needed to capture the point load acting on the substrate surface $\partial\mathcal{B}$, since now $\boldsymbol{t}_{\mathrm{SL}}$ and $\boldsymbol{t}_{\mathrm{SG}}$ can only balance the horizontal component of $\boldsymbol{t}_{\mathrm{LG}}$ (Young's equilibrium). If the droplet is not pinned along $\mathcal{C}$, $\epsilon\, \tilde{\boldsymbol{\sigma}} \boldsymbol{n}$ is normal to $\partial\mathcal{B}$.

Also, weak form (76) simplifies in view of (100): We now have

$$\begin{aligned} 0 \ = \ & \int_{\mathcal{S}_{\mathrm{L}}} \left[\sigma^{\alpha\beta}\, \delta x_{\alpha;\beta} - \sigma^{\alpha\beta}\, b_{\alpha\beta}\, \delta x - \left(p_{\mathrm{f}}\, \boldsymbol{n} + \bar{\boldsymbol{f}} \right) \cdot \delta \boldsymbol{x} \right] \mathrm{d}a - \int_{\partial_t \mathcal{S}_{\mathrm{L}}} \bar{\boldsymbol{t}} \cdot \delta \boldsymbol{x}\, \mathrm{d}a \\ & - \int_{\mathcal{S}_{\mathrm{c}}} \boldsymbol{f}_{\mathrm{c}} \cdot \delta \boldsymbol{x}\, \mathrm{d}a - \int_{\mathcal{C}} \boldsymbol{q}_{\mathrm{c}} \cdot \delta \boldsymbol{x}\, \mathrm{d}s \ . \end{aligned} \tag{105}$$

Here, p_{f} is viewed as an external force on interface $\mathcal{S}_{\mathrm{L}}$ that is given by (100). The consequences of this revision are discussed in Sec. 4.4. The quantity p_{v} is indeterminate from equilibrium and must remain related to the incompressibility constraint (13). Treating p_{v} as the Lagrange multiplier associated with this constraint, δp_{f} now corresponds to δp_{v}, which is constant across $\mathcal{D}$. Eq. (71) now reads

$$\delta_{p_{\mathrm{f}}} \hat{\Pi} = \delta p_{\mathrm{v}} \int_{\mathcal{D}_0} g_{\mathrm{v}}\, \mathrm{d}V = \delta p_{\mathrm{v}} \big(V_0 - V \big) = 0 \quad \forall\ \delta p_{\mathrm{v}} \in \mathcal{P}_{\mathrm{v}} \ , \tag{106}$$

where

$$V = \int_{\mathcal{D}} \mathrm{d}v = \frac{1}{3} \int_{\partial\mathcal{D}} \boldsymbol{x} \cdot \boldsymbol{n}\, \mathrm{d}a \tag{107}$$

and

$$V_0 = \int_{\mathcal{D}_0} \mathrm{d}V = \frac{1}{3} \int_{\partial\mathcal{D}_0} \boldsymbol{X} \cdot \boldsymbol{N}\, \mathrm{d}A \tag{108}$$

denote the volume of $\mathcal{D}_0$ and $\mathcal{D}$. This implies that now the global incompressibility constraint

$$\hat{g}_{\mathrm{v}} = V_0 - V = 0 \tag{109}$$

is enforced. The reduced system is now governed by the two coupled weak equilibrium equations (77) and (105), the weak constraints (71)–(75), and the strong constraint (109). The elimination of unknown p_{f} at this stage[7] leads to an unsymmetric formulation as is seen in Sec. 4.4. For this reason, the unsymmetry stemming from the variational inconsistency introduced by (66), also seen in Sec. 4.4, does not introduce any further disadvantage.

3.9 The solution of the Euler-Lagrange equations

The Euler-Lagrange equations given above can be solved in general by numerical methods, that are for example based on the weak form equations (76), (77) and (105); e.g. see [18].

[7] After variation and before linearization.

Numerical methods are not discussed here, although an example is shown for illustration in Sec. 5. Analytical solutions, on the other hand, can only be found for special cases. One of these is the case where we have no external loading ($\bar{\boldsymbol{b}} = \boldsymbol{0}$, $\bar{\boldsymbol{f}} = \bar{f}^\alpha \boldsymbol{a}_\alpha + \bar{p}\,\boldsymbol{n} = \boldsymbol{0}$ and $\bar{\boldsymbol{t}} = \boldsymbol{0}$), constant surface tension according to (53) (so that $\sigma^{\alpha\beta}{}_{;\beta} = 0$ and $\sigma^{\alpha\beta} b_{\alpha\beta} = \gamma\, b^\alpha_\alpha$), and a stiff substrate that obeys small deformation theory. In this case, the substrate surface $\mathcal{S}_\mathrm{S}$ remains flat, so that $b^\alpha_\alpha = 0$, and the droplet surface $\mathcal{S}_\mathrm{LG}$ attains a spherical shape. The mean curvature of the sphere is $b^\alpha_\alpha = -2/R_0$, where R_0 denotes the radius. The fluid pressure, constant within $\mathcal{D}$, thus is $p_\mathrm{f} = 2\gamma_\mathrm{LG}/R_0$ according to (87). On $\mathcal{S}_\mathrm{SL}$ we then find the contact pressure $p_\mathrm{c} = p_\mathrm{f}$ and contact shear $f^\alpha_\mathrm{c} = 0$ according to (89) and (90). The contact radius depends on the droplet volume and the contact angle at $\mathcal{C}$, which in turn depends on the three surface tensions. If the contact line is not pinned, the line force $\epsilon\, \tilde{\boldsymbol{\sigma}} \boldsymbol{n}$ is normal to the substrate surface, and one can obtain the relations

$$\begin{aligned} \gamma_\mathrm{SG} - \gamma_\mathrm{SL} &= \gamma_\mathrm{LG} \cos\theta_\mathrm{c} \ , \\ \epsilon\, \tilde{\sigma} &= \gamma_\mathrm{LG} \sin\theta_\mathrm{c} \ , \end{aligned} \tag{110}$$

from (104). Using the half-space solution of Bousinesq and Cerutti [19] one may then compute the stress state $\tilde{\boldsymbol{\sigma}}$ due to the line load and contact pressure.

4 Linearization of the governing equations

This section presents the linearization of the governing weak forms. Both the full system (Sec. 3.7) and the reduced (Sec. 3.8) system are discussed. From the linearization, the tangent of the system is found, which allows an assessment of the system's stability. The linearization is further needed for certain numerical descriptions of the system. In particular, the consequences of the reduction are illustrated.

Consider a state of the system, characterized by the variable $\mathbf{y} = [\boldsymbol{x},\, p_\mathrm{f},\, p_\mathrm{c},\, \tau_\alpha,\, q,\, q_\alpha]$. Further consider a change of this state, denoted $\Delta\mathbf{y} = [\Delta\boldsymbol{x},\, \Delta p_\mathrm{f},\, \Delta p_\mathrm{c},\, \Delta\tau_\alpha,\, \Delta q,\, \Delta q_\alpha]$. The linearization of variation $\delta\Pi$ at this state in the direction of the considered change, is written as

$$\delta\Pi(\mathbf{y} + \Delta\mathbf{y}) = \delta\Pi(\mathbf{y}) + \Delta\delta\Pi(\mathbf{y}) \ . \tag{111}$$

Now, before examining the change $\Delta\delta\Pi$, we discuss the linearization of kinematical quantities and constitutive relations.

4.1 Linearization of various kinematical quantities

The determination of the change is analogous to the determination of the variation. The changes $\Delta\tilde{J}$, $\Delta\boldsymbol{a}_\alpha$, $\Delta a_{\alpha\beta}$, ΔJ, $\Delta\boldsymbol{n}$, $\Delta\boldsymbol{a}^\alpha$, $\Delta a^{\alpha\beta}$, $\Delta\lambda_\mathrm{c}$, $\Delta(\boldsymbol{x}_\mathrm{p})$, Δg_n and $\Delta g^\alpha_\mathrm{t} = \Delta\xi^\alpha_\mathrm{p}$ are thus given in analogy to the expressions of Sec. 3.2. What remains to be determined are the changes of the variations. Some of these are easily determined or of minor importance. Those that are neither are provided in the following.

The change of variation δJ is given by

$$\Delta\delta J = J\, \delta\boldsymbol{a}_\alpha \cdot \left(a^{\alpha\beta}\, \boldsymbol{n}\otimes\boldsymbol{n} + \boldsymbol{a}^\alpha \otimes \boldsymbol{a}^\beta - \boldsymbol{a}^\beta \otimes \boldsymbol{a}^\alpha\right) \Delta\boldsymbol{a}_\beta \ , \tag{112}$$

according to (27) and (29), while $\Delta\delta\lambda_\mathrm{c}$ is

$$\Delta\delta\lambda_\mathrm{c} = \frac{1}{\lambda_\mathrm{c}}\, \Delta\boldsymbol{a}_\mathrm{c} \cdot \delta\boldsymbol{a}_\mathrm{c} - \frac{1}{\lambda_\mathrm{c}^3} (\Delta\boldsymbol{a}_\mathrm{c} \cdot \boldsymbol{a}_\mathrm{c})(\boldsymbol{a}_\mathrm{c} \cdot \delta\boldsymbol{a}_\mathrm{c}) \ , \tag{113}$$

according to (35). For a dependent quantity, like $\boldsymbol{x}_\mathrm{p} = \boldsymbol{x}(\xi^\alpha_\mathrm{p})$, we find

$$\Delta\delta(\boldsymbol{x}_\mathrm{p}) = \delta\boldsymbol{a}^\mathrm{p}_\alpha\,\Delta\xi^\alpha_\mathrm{p} + \Delta\boldsymbol{a}^\mathrm{p}_\alpha\,\delta\xi^\alpha_\mathrm{p} + \delta\xi^\alpha_\mathrm{p}\,\boldsymbol{a}^\mathrm{p}_{\alpha,\beta}\,\Delta\xi^\beta_\mathrm{p} + \boldsymbol{a}^\mathrm{p}_\alpha\,\Delta\delta\xi^\alpha_\mathrm{p}\ . \tag{114}$$

Similar expressions follow for $\Delta\delta(\boldsymbol{a}^\mathrm{p}_\alpha)$ and $\Delta\delta(\boldsymbol{n}_\mathrm{p})$. The changes of the contact quantities δg_n and δg_t can then be determined as [3; 4]

$$\begin{aligned}\Delta\delta g_\mathrm{n} \;=\; & -\boldsymbol{n}_\mathrm{p}\cdot\Big(\delta\boldsymbol{a}^\mathrm{p}_\alpha\,\Delta\xi^\alpha_\mathrm{p} + \Delta\boldsymbol{a}^\mathrm{p}_\alpha\,\delta\xi^\alpha_\mathrm{p} + \delta\xi^\alpha_\mathrm{p}\,\boldsymbol{a}^\mathrm{p}_{\alpha,\beta}\,\Delta\xi^\beta_\mathrm{p}\Big)\\ & +\; g_\mathrm{n}\,\boldsymbol{n}_\mathrm{p}\cdot\Big(\delta\boldsymbol{a}^\mathrm{p}_\alpha + \boldsymbol{a}^\mathrm{p}_{\alpha,\gamma}\,\delta\xi^\gamma_\mathrm{p}\Big)\,a^{\alpha\beta}_\mathrm{p}\,\Big(\Delta\boldsymbol{a}^\mathrm{p}_\beta + \boldsymbol{a}^\mathrm{p}_{\beta,\delta}\,\Delta\xi^\delta_\mathrm{p}\Big)\cdot\boldsymbol{n}_\mathrm{p}\end{aligned} \tag{115}$$

and, by examining $\Delta\delta f_\alpha$ from (18),

$$\begin{aligned}\Delta\delta\xi^\alpha_\mathrm{p} = c^{\alpha\beta}_\mathrm{p}\Big[\; & -\boldsymbol{a}^\mathrm{p}_\beta\cdot\Big(\delta\boldsymbol{a}^\mathrm{p}_\gamma\,\Delta\xi^\gamma_\mathrm{p} + \Delta\boldsymbol{a}^\mathrm{p}_\gamma\,\delta\xi^\gamma_\mathrm{p} + \delta\xi^\gamma_\mathrm{p}\,\boldsymbol{a}^\mathrm{p}_{\gamma,\delta}\,\Delta\xi^\delta_\mathrm{p}\Big)\\ & +\; g_\mathrm{n}\,\boldsymbol{n}_\mathrm{p}\cdot\Big(\delta\boldsymbol{a}^\mathrm{p}_{\beta,\gamma}\,\Delta\xi^\gamma_\mathrm{p} + \Delta\boldsymbol{a}^\mathrm{p}_{\beta,\gamma}\,\delta\xi^\gamma_\mathrm{p} + \delta\xi^\gamma_\mathrm{p}\,\boldsymbol{a}^\mathrm{p}_{\beta,\gamma\delta}\,\Delta\xi^\delta_\mathrm{p}\Big)\\ & -\; \boldsymbol{a}^\mathrm{p}_\gamma\cdot\Big(\delta\boldsymbol{a}^\mathrm{p}_\beta\,\Delta\xi^\gamma_\mathrm{p} + \Delta\boldsymbol{a}^\mathrm{p}_\beta\,\delta\xi^\gamma_\mathrm{p} + \delta\xi^\gamma_\mathrm{p}\,\boldsymbol{a}^\mathrm{p}_{\beta,\delta}\,\Delta\xi^\delta_\mathrm{p} + \delta\xi^\delta_\mathrm{p}\,\boldsymbol{a}^\mathrm{p}_{\beta,\delta}\,\Delta\xi^\gamma_\mathrm{p}\Big)\\ & +\; (\delta\boldsymbol{x} - \delta\boldsymbol{x}_\mathrm{p})\cdot\Big(\Delta\boldsymbol{a}^\mathrm{p}_\beta + \boldsymbol{a}^\mathrm{p}_{\beta,\gamma}\,\Delta\xi^\gamma_\mathrm{p}\Big) + (\Delta\boldsymbol{x} - \Delta\boldsymbol{x}_\mathrm{p})\cdot\Big(\delta\boldsymbol{a}^\mathrm{p}_\beta + \boldsymbol{a}^\mathrm{p}_{\beta,\gamma}\,\delta\xi^\gamma_\mathrm{p}\Big)\Big]\ .\end{aligned} \tag{116}$$

At equilibrium the expressions for δg_n and δg_t simplify to those given in (41) and (42), which allow an identification of the contact forces in (64) and (65). If one chooses to work with this simplification, linearizing $\delta\hat{g}_\mathrm{n}$ and $\delta\hat{g}_\mathrm{t}$ with disregard to their derivation, one finds

$$\Delta\delta\hat{g}_\mathrm{n} = \Delta(\delta\hat{g}_\mathrm{n}) = -\boldsymbol{n}_\mathrm{p}\cdot\Big(\delta\boldsymbol{a}^\mathrm{p}_\alpha\,\Delta\xi^\alpha_\mathrm{p} + \Delta\boldsymbol{a}^\mathrm{p}_\alpha\,\delta\hat{\xi}^\alpha_\mathrm{p} + \hat{\delta}\xi^\alpha_\mathrm{p}\,\boldsymbol{a}^\mathrm{p}_{\alpha,\beta}\,\Delta\xi^\beta_\mathrm{p}\Big) \tag{117}$$

and

$$\begin{aligned}\Delta\delta\hat{\xi}^\alpha_\mathrm{p} = \Delta(\delta\hat{\xi}^\alpha_\mathrm{p}) = a^{\alpha\beta}_\mathrm{p}\Big[\; & -\boldsymbol{a}^\mathrm{p}_\beta\cdot\Big(\delta\boldsymbol{a}^\mathrm{p}_\gamma\,\Delta\xi^\gamma_\mathrm{p} + \Delta\boldsymbol{a}^\mathrm{p}_\gamma\,\delta\hat{\xi}^\gamma_\mathrm{p} + \hat{\delta}\xi^\gamma_\mathrm{p}\,\boldsymbol{a}^\mathrm{p}_{\gamma,\delta}\,\Delta\xi^\delta_\mathrm{p}\Big)\\ & -\; \boldsymbol{a}^\mathrm{p}_\gamma\cdot\Big(\Delta\boldsymbol{a}^\mathrm{p}_\beta\,\hat{\delta}\xi^\gamma_\mathrm{p} + \delta\hat{\xi}^\gamma_\mathrm{p}\,\boldsymbol{a}^\mathrm{p}_{\beta,\delta}\,\Delta\xi^\delta_\mathrm{p}\Big)\\ & +\; (\delta\boldsymbol{x} - \delta\boldsymbol{x}_\mathrm{p})\cdot\Big(\Delta\boldsymbol{a}^\mathrm{p}_\beta + \boldsymbol{a}^\mathrm{p}_{\beta,\gamma}\,\Delta\xi^\gamma_\mathrm{p}\Big)\Big]\ .\end{aligned} \tag{118}$$

These expressions contain only a subset of the terms appearing in (115) and (116). But they are not symmetric w.r.t. linearization and variation.

4.2 Linearization of the stress measures

We now discuss the linearization of stress measures $\tilde{\boldsymbol{\sigma}}$, p_f and $\sigma^{\alpha\beta}$ that characterize the constitutive behavior of the system. The Cauchy stress in $\mathcal{B}$ can be linearized through

$$\Delta\tilde{\sigma}_{ij} = \frac{\partial\tilde{\sigma}_{ij}}{\partial\tilde{e}_{k\ell}}\,\Delta\tilde{e}_{kl}\ . \tag{119}$$

where $e_{k\ell}$ are the components[8] of the Green-Almansi strain tensor $\tilde{\boldsymbol{e}} = \frac{1}{2}\big(\tilde{\boldsymbol{I}} - \tilde{\boldsymbol{F}}^{-T}\tilde{\boldsymbol{F}}^{-1}\big)$. The elasticity tensor

$$\tilde{c}_{ijk\ell} = \frac{\partial\tilde{\sigma}_{ij}}{\partial\tilde{e}_{k\ell}} \tag{120}$$

[8]Latin symbols are used for indices running from 1 to 3.

follows from the type of constitutive model chosen for $\mathcal{B}$. This is not discussed further here. For compressible fluid behavior in $\mathcal{D}$ the fluid pressure can be linearized through

$$\Delta p_{\mathrm{f}} = \frac{\partial p_{\mathrm{f}}}{\partial \tilde{J}}\,\Delta\tilde{J}\ , \tag{121}$$

where

$$K := -\frac{\partial p_{\mathrm{f}}}{\partial \tilde{J}} = \frac{\partial^2 \mathcal{W}_{\mathcal{D}}}{\partial \tilde{J}^2} \tag{122}$$

is the bulk modulus of the fluid. The membrane stress $\tau^{\alpha\beta} = J\,\sigma^{\alpha\beta}$, considered for convenience, can be linearized through

$$\Delta\tau^{\alpha\beta} = \frac{\partial \tau^{\alpha\beta}}{\partial a_{\gamma\delta}}\Delta a_{\gamma\delta}\ . \tag{123}$$

The tensor

$$c^{\alpha\beta\gamma\delta} := 2\frac{\partial \tau^{\alpha\beta}}{\partial a_{\gamma\delta}} \tag{124}$$

denotes the elasticity tensor for the membrane. For the three examples in Sec. 3.4 one finds

$$c^{\alpha\beta\gamma\delta} = \gamma J\Big(\frac{1}{a}\big(e^{\alpha\gamma}e^{\beta\delta} + e^{\alpha\delta}e^{\beta\gamma}\big) - a^{\alpha\beta}a^{\gamma\delta}\Big) \tag{125}$$

for stress (53),

$$c^{\alpha\beta\gamma\delta} = \mu\Big(2a^{\alpha\beta}a^{\gamma\delta} - \frac{1}{a}\big(e^{\alpha\gamma}e^{\beta\delta} + e^{\alpha\delta}e^{\beta\gamma}\big)\Big) \tag{126}$$

for stress (55), and

$$c^{\alpha\beta\gamma\delta} = \mu J^{-2}\Big(4a^{\alpha\beta}a^{\gamma\delta} - \frac{1}{a}\big(e^{\alpha\gamma}e^{\beta\delta} + e^{\alpha\delta}e^{\beta\gamma}\big)\Big) \tag{127}$$

for stress (60). We note that in the first case – the case of liquids – the elasticity tensor is not positive definite, since

$$m_{\alpha\beta}\,c^{\alpha\beta\gamma\delta}\,m_{\gamma\delta} > 0 \quad \forall\, m_{\alpha\beta} \neq 0 \tag{128}$$

is not satisfied. E.g. taking $m_{\alpha\beta} = a_{\alpha\beta}$ yields $m_{\alpha\beta}\,c^{\alpha\beta\gamma\delta}\,m_{\gamma\delta} = -8J\gamma$.

4.3 Linearization of the full system

With the relations of the preceding two sections, the change $\Delta\delta\Pi$ can now be evaluated. It is seen that this quantity is symmetric w.r.t. linearization and variation. The change of $\delta\Pi_{\mathrm{int}\mathcal{B}}$ gives the well-known result [20]

$$\Delta\delta\Pi_{\mathrm{int}\mathcal{B}} = \int_{\mathcal{B}} \delta x_{i,j}\,\tilde{\sigma}_{jk}\,\Delta x_{i,k}\,\mathrm{d}v + \int_{\mathcal{B}} \delta x_{i,j}\,\tilde{c}_{ijk\ell}\,\Delta x_{k,\ell}\,\mathrm{d}v\ . \tag{129}$$

The change of $\delta\Pi_{\mathrm{int}\mathcal{D}}$ simply gives

$$\Delta\delta\Pi_{\mathrm{int}\mathcal{D}} = \int_{\mathcal{D}} p_{\mathrm{f}}\,\mathrm{div}\,\delta\boldsymbol{x}\ \mathrm{div}\,\Delta\boldsymbol{x}\,\mathrm{d}v - \int_{\mathcal{D}} \delta p_{\mathrm{f}}\,\mathrm{div}\,\Delta\boldsymbol{x}\,\mathrm{d}v - \int_{\mathcal{D}} \Delta p_{\mathrm{f}}\,\mathrm{div}\,\delta\boldsymbol{x}\,\mathrm{d}v\ , \tag{130}$$

for the incompressible case, and

$$\Delta\delta\Pi_{\mathrm{int}\mathcal{D}} = \int_{\mathcal{D}} p_{\mathrm{f}}\,\mathrm{div}\,\delta\boldsymbol{x}\ \mathrm{div}\,\Delta\boldsymbol{x}\,\mathrm{d}v + \int_{\mathcal{D}} K\,\mathrm{div}\,\delta\boldsymbol{x}\ \mathrm{div}\,\Delta\boldsymbol{x}\,\mathrm{d}v\ , \tag{131}$$

for the compressible case. To linearize $\delta\Pi_{\text{int}\mathcal{S}}$, first note that since $\delta x_{\alpha;\beta} = \delta \boldsymbol{x}_{;\beta} \cdot \boldsymbol{a}_\alpha + \delta x\, b_{\alpha\beta}$ one can write

$$\delta\Pi_{\text{int}\mathcal{S}} = \int_{\mathcal{S}_0} \delta \boldsymbol{x}_{;\alpha} \cdot \tau^{\alpha\beta}\, \boldsymbol{a}_\beta \,\mathrm{d}A \ . \tag{132}$$

We thus obtain

$$\Delta\delta\Pi_{\text{int}\mathcal{S}} = \int_{\mathcal{S}_0} \delta \boldsymbol{x}_{;\alpha} \cdot \Delta\tau^{\alpha\beta}\, \boldsymbol{a}_\beta \,\mathrm{d}A + \int_{\mathcal{S}_0} \delta \boldsymbol{x}_{;\alpha} \cdot \tau^{\alpha\beta}\, \Delta\boldsymbol{a}_\beta \,\mathrm{d}A \ . \tag{133}$$

Inserting $\Delta\tau^{\alpha\beta}$ and $\Delta a_{\gamma\delta}$ from above, yields

$$\Delta\delta\Pi_{\text{int}\mathcal{S}} = \int_{\mathcal{S}_0} c^{\alpha\beta\gamma\delta}\, \delta \boldsymbol{x}_{,\alpha}\, (\boldsymbol{a}_\beta \otimes \boldsymbol{a}_\gamma)\, \Delta \boldsymbol{x}_{,\delta} \,\mathrm{d}A + \int_{\mathcal{S}_0} \delta \boldsymbol{x}_{,\alpha} \cdot \tau^{\alpha\beta}\, \Delta\boldsymbol{x}_{,\beta} \,\mathrm{d}A \ . \tag{134}$$

The linearization of the contact variation $\delta\Pi_{\text{c}}$ in (61) is straight forward, but yields many different terms. For conciseness, we only list the 8 terms emanating from p_{c}. This gives

$$\begin{aligned} \Delta\delta\Pi_{\text{c}} = &- \int_{\mathcal{S}_{\text{c}}} p_{\text{c}}\, \Delta\delta g_{\text{n}} \,\mathrm{d}a - \int_{\mathcal{S}_{\text{c}}} \left(\Delta p_{\text{c}}\, \delta g_{\text{n}} + \delta p_{\text{c}}\, \Delta g_{\text{n}}\right) \mathrm{d}a - \int_{\mathcal{S}_{\text{c}}} p_{\text{c}}\, g_{\text{n}}\, \frac{\Delta\delta J}{J} \,\mathrm{d}a \\ &- \int_{\mathcal{S}_{\text{c}}} p_{\text{c}} \left(\delta g_{\text{n}}\, \frac{\Delta J}{J} + \Delta g_{\text{n}}\, \frac{\delta J}{J}\right) \mathrm{d}a - \int_{\mathcal{S}_{\text{c}}} g_{\text{n}} \left(\Delta p_{\text{c}}\, \frac{\delta J}{J} + \delta p_{\text{c}}\, \frac{\Delta J}{J}\right) \mathrm{d}a + \dots \ . \end{aligned} \tag{135}$$

The remaining 24 terms, emanating from τ_α, q and q_α, look very similar. Here, contributions $\Delta\delta g_{\text{n}}$, $\Delta\delta g_{\text{t}}^\alpha$, $\Delta\delta J$ and $\Delta\delta\lambda_{\text{c}}$ are given in Sec. 4.1. Note, that several terms vanish in $\Delta\delta\Pi_{\text{c}}$ at equilibrium where $g_{\text{n}} = g_{\text{t}}^\alpha = 0$.
The last contribution, the change of $\delta\Pi_{\text{ext}}$ is simply

$$\Delta\delta\Pi_{\text{ext}} = 0 \ . \tag{136}$$

The complete linearization of the weak form is then characterized by the change

$$\Delta\delta\Pi = \Delta\delta\Pi_{\text{int}\mathcal{B}} + \Delta\delta\Pi_{\text{int}\mathcal{D}} + \Delta\delta\Pi_{\text{int}\mathcal{S}} + \Delta\delta\Pi_{\text{c}} \ . \tag{137}$$

4.4 Linearization of the reduced system

The reduced system, presented in Sec. 3.8 is computationally interesting since it is more efficient than the full system. However, its linearization turns out to be unsymmetric, since the subsequent linearization is treated differently than the initial variation. For the reduced system the fluid pressure p_{f} is treated as an external force in (105). The linearization of this contribution yields

$$\Delta\delta\hat{\Pi}_{\text{ext}} = -\int_{\mathcal{S}_{\text{L}}} \delta\boldsymbol{x} \cdot \Delta p_{\text{f}}\, \boldsymbol{n} \,\mathrm{d}a - \int_{\mathcal{S}_{\text{L}}} \delta\boldsymbol{x} \cdot p_{\text{f}}\, \Delta(\boldsymbol{n} \,\mathrm{d}a) \ . \tag{138}$$

Here we have

$$\Delta p_{\text{f}} = \Delta p_{\text{v}} + \Delta\boldsymbol{x} \cdot \rho\, \bar{\boldsymbol{b}} \ , \tag{139}$$

due to (100), and

$$\Delta(\boldsymbol{n} \,\mathrm{d}a) = \left(\boldsymbol{n} \otimes \boldsymbol{a}^\alpha - \boldsymbol{a}^\alpha \otimes \boldsymbol{n}\right) \Delta\boldsymbol{a}_\alpha \,\mathrm{d}a \ , \tag{140}$$

due to (27) and (28). The linearization of contribution $\delta_{p_{\text{f}}}\hat{\Pi}$, appearing in (106), gives

$$\Delta\delta_{p_{\text{f}}}\hat{\Pi} = -\delta p_{\text{v}}\, \Delta V \ , \tag{141}$$

with

$$\Delta V = \frac{1}{3}\int_{\mathcal{S}_{\text{L}}} \Delta\boldsymbol{x} \cdot \boldsymbol{n} \,\mathrm{d}a + \frac{1}{3}\int_{\mathcal{S}_{\text{L}}} \boldsymbol{x} \cdot \Delta(\boldsymbol{n} \,\mathrm{d}a) \ . \tag{142}$$

If surface $\mathcal{S}_\mathrm{L}$ is closed, or if $\Delta\boldsymbol{x} = \boldsymbol{0}$ on the boundary $\partial\mathcal{S}_\mathrm{L}$, we have (see Appendix B)

$$\int_{\mathcal{S}_\mathrm{L}} \boldsymbol{x} \cdot (\boldsymbol{n} \otimes \boldsymbol{a}^\alpha - \boldsymbol{a}^\alpha \otimes \boldsymbol{n})\, \Delta\boldsymbol{a}_\alpha \,\mathrm{d}a = 2 \int_{\mathcal{S}_\mathrm{L}} \Delta\boldsymbol{x} \cdot \boldsymbol{n} \,\mathrm{d}a \;, \tag{143}$$

such that

$$\Delta\delta_{p_\mathrm{f}}\hat{\Pi} = -\delta p_\mathrm{v} \int_{\mathcal{S}_\mathrm{L}} \Delta\boldsymbol{x} \cdot \boldsymbol{n} \,\mathrm{d}a \tag{144}$$

in this case. This part is symmetric to the first term of $\Delta\delta\hat{\Pi}_\mathrm{ext}$. But due to the second term in $\Delta\delta\hat{\Pi}_\mathrm{ext}$, the linearization of the reduced weak form remains unsymmetric. Therefore nothing is lost if the contact contribution is also considered in the simplified version of expression (66). For this we find

$$\Delta\delta\hat{\Pi}_\mathrm{c} = -\int_{\mathcal{S}_\mathrm{c}} p_\mathrm{c}\, \Delta\delta\hat{g}_\mathrm{n} \,\mathrm{d}a - \int_{\mathcal{S}_\mathrm{c}} \left(\Delta p_\mathrm{c}\, \delta\hat{g}_\mathrm{n} + \delta p_\mathrm{c}\, \Delta g_\mathrm{n}\right) \mathrm{d}a - \int_{\mathcal{S}_\mathrm{c}} \left(p_\mathrm{c}\, \hat{\delta} g_\mathrm{n} + g_\mathrm{n}\, \delta p_\mathrm{c}\right) \frac{\Delta J}{J} \,\mathrm{d}a + \ldots \tag{145}$$

The complete linearization of the reduced weak form is then characterized by the change

$$\Delta\delta\Pi = \Delta\delta\Pi_{\mathrm{int}\mathcal{B}} + \Delta\delta_{p_\mathrm{f}}\hat{\Pi} + \Delta\delta\Pi_{\mathrm{int}\mathcal{S}} + \Delta\delta\hat{\Pi}_\mathrm{c} - \Delta\delta\hat{\Pi}_\mathrm{ext} \;. \tag{146}$$

5 A computational example

To give an impression of the scope of applications of the presented model equations, we briefly discuss a computational example. Consider a liquid droplet, $\mathcal{D}$, in quasi-static contact with a deformable substrate block $\mathcal{B}$. The system is analyzed by a finite element discretization of the reduced formulation given in Secs. 3.8 and 4.4. The substrate is discretized by hexahedral elements. In the bulk, linear 8-noded elements are used. On the upper substrate surface (i.e. on $\mathcal{S}_\mathrm{S}$), quadratically enriched surface elements, with 13 nodes, are used [21]. The interfaces are modeled by the stabilized membrane formulation of [18]. A suitable computational contact algorithm for line contact on deformable substrates has not been developed yet. Therefore the contact line $\mathcal{C}$ is assumed to be pinned on $\mathcal{B}$ in the example. Then, no contact algorithm is required. This corresponds to adding weak forms (77) and (105), thus eliminating the contact integrals over $\mathcal{S}_\mathrm{c}$ and $\mathcal{C}$. In the undeformed configuration the block $\mathcal{B}$ has the dimension $2L_0 \times 2L_0 \times L_0$. The droplet has the volume $2L_0^3$. $\mathcal{C}$ is pinned at the radius L_0. A Neo-Hookean material model is considered for $\mathcal{B}$ with the constants $E = E_0$ and $\nu = 0.3$. The surface tension of all interfaces is considered constant, using $\gamma_\mathrm{LG} = 0.08\, E_0 L_0$, $\gamma_\mathrm{SL} = 0.10\, E_0 L_0$ and $\gamma_\mathrm{SG} = 0.04\, E_0 L_0$. A constant body force acts on the medium enclosed by the droplet considering $\rho\bar{\boldsymbol{b}} = -0.2\, E_0/L_0\, [\sin\alpha,\, 0,\, \cos\alpha]^T$ with $\alpha = 20°$. This corresponds to a droplet under gravity on an inclined substrate. Fig. 3 shows the finite element solution for the given parameters. It can be seen that large deformations appear in the system, leading to a distinct wetting ridge along $\mathcal{C}$.

6 Conclusion

This paper presents the governing equations of filled liquid and solid membranes in contact with a deformable substrates. An example are liquid droplets on soft substrates. Apart from considering quasi-static conditions, the problem is treated very general: It includes compressible and incompressible liquids, general hyperelastic membrane models that may contain internal constraints, and general hyperelastic substrates. It also includes two different treatments of

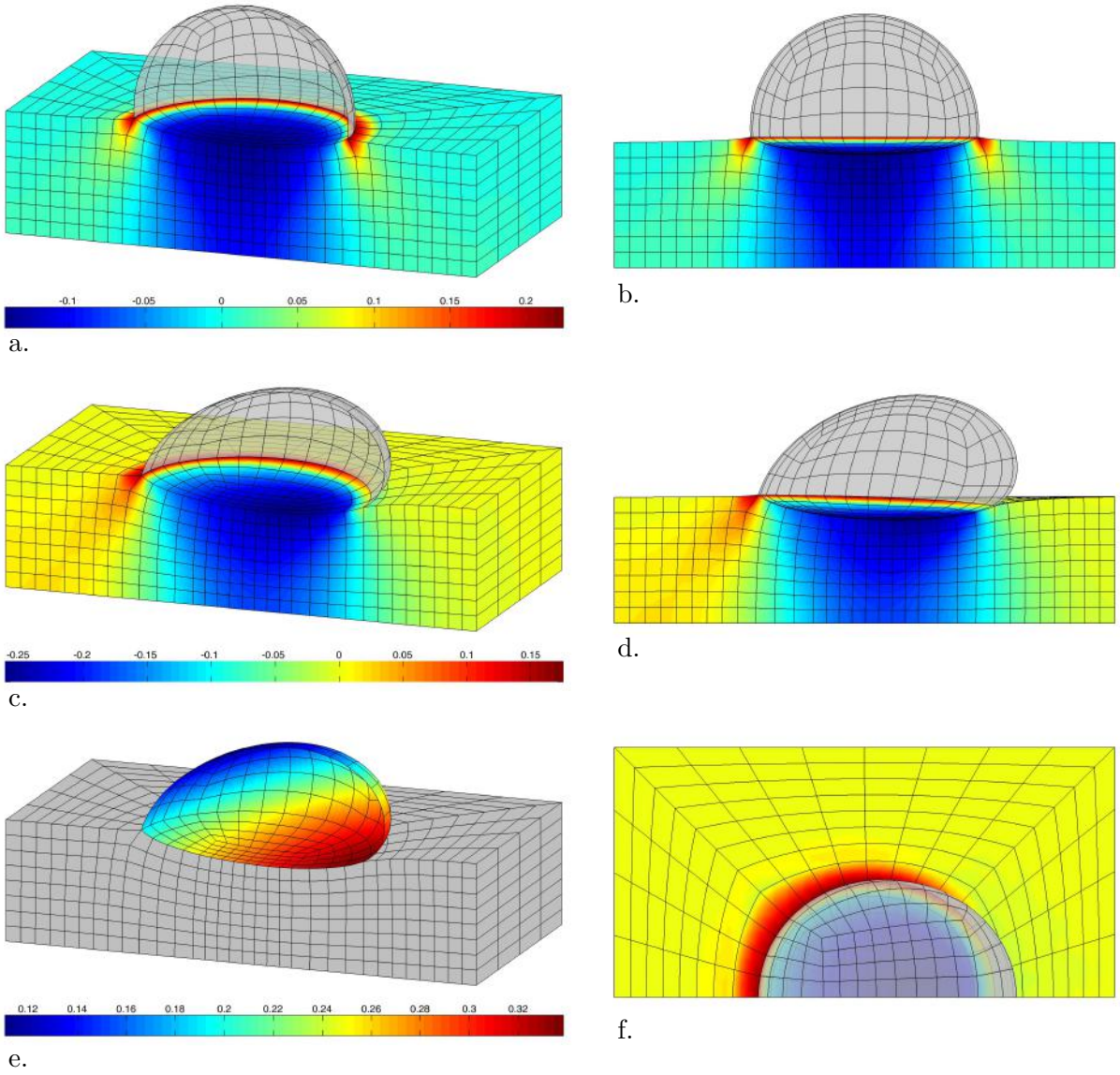

Figure 3: Contact between a liquid droplet and a deformable substrate: a)–b) reference solution for $\|\rho\bar{\boldsymbol{b}}\| = 0$; c)–f) solution for $\|\rho\bar{\boldsymbol{b}}\| = 0.2\,E_0/L_0$; the coloring in e) shows the pressure p_f/E_0 acting on $\mathcal{S}_\mathrm{L}$; otherwise the coloring shows the vertical stress component $\tilde{\sigma}_{33}/E_0$ within $\mathcal{B}$.

the wetting ridge that appears at the three phase boundary: a detailed microscopic and a coarse-scale macroscopic viewpoint. The contact between membrane and substrate is formulated considering distinct contact constraints for the contact surface $\mathcal{S}_\mathrm{c}$ and the contact line $\mathcal{C}$. The considered setup is governed by a global potential Π. It is shown that the governing equilibrium and constraint equations follow as the Euler-Lagrange equations of this potential. It is further shown how these can be simplified into a reduced set of equations that is convenient for computational approaches. For both sets, the full system and the reduced system, the linearization is then derived.
The present model formulation is suitable for numerical solution approaches like the finite element method. A corresponding example that does not require the contact contributions is briefly discussed. Concerning contact, a FE implementation of the model has been considered for rigid substrates and without sticking contact [18]. The extension of this implementation to the full problem requires a suitable algorithm for line contact, which will be considered in future work.

A Constrained membrane elasticity

For a constrained elastic body $\mathcal{B}$, the first Piola-Kirchhoff stress follows from

$$\boldsymbol{P} = \frac{\partial \hat{W}_\mathcal{B}}{\partial \tilde{\boldsymbol{F}}} \ , \quad \hat{W}_\mathcal{B} = W_\mathcal{B} + q_\mathcal{B}\, g_\mathcal{B} \ , \tag{147}$$

where $W_\mathcal{B} = W_\mathcal{B}(\tilde{\boldsymbol{F}})$ and $g_\mathcal{B} = g_\mathcal{B}(\tilde{\boldsymbol{F}})$ are the energy density (per reference volume) and the constraint of body $\mathcal{B}$; $q_\mathcal{B}$ corresponds to the Lagrange multiplier. Within a membrane, the bulk deformation gradient takes the form

$$\tilde{\boldsymbol{F}} = \boldsymbol{F} + \lambda_3\, \boldsymbol{n} \otimes \boldsymbol{N} \ , \tag{148}$$

where $\boldsymbol{F} = \boldsymbol{a}_\alpha \otimes \boldsymbol{A}^\alpha$ is the in-plane deformation gradient. Considering

$$\Delta \hat{W}_\mathcal{B} = \frac{\partial \hat{W}_\mathcal{B}}{\partial \tilde{\boldsymbol{F}}} : \Delta \tilde{\boldsymbol{F}} \ , \tag{149}$$

$\boldsymbol{P} = \tilde{J}\, \tilde{\boldsymbol{\sigma}}\, \tilde{\boldsymbol{F}}^{-T}$ and $\tilde{\boldsymbol{\sigma}} = \boldsymbol{\sigma}/t + \tilde{\sigma}_{33}\, \boldsymbol{n} \otimes \boldsymbol{n}$, where t is the current thickness of the membrane, one can derive

$$\Delta \hat{W}_\mathcal{B} = \frac{J}{2T}\, \sigma^{\alpha\beta}\, \Delta a_{\alpha\beta} + J\, \tilde{\sigma}_{33}\, \Delta \lambda_3 \ , \tag{150}$$

where $T = t/\lambda_3$ is the reference thickness of the membrane. Introducing the energy density (per reference surface area)

$$\hat{W}_\mathcal{S} = \hat{W}_\mathcal{B}\, T = W_\mathcal{S} + q_\mathcal{S}\, g_\mathcal{B} \ , \quad W_\mathcal{S} = W_\mathcal{B}\, T \ , \quad q_\mathcal{S} = q_\mathcal{B}\, T \ , \tag{151}$$

for which we can write

$$\Delta \hat{W}_\mathcal{S} = \frac{\partial \hat{W}_\mathcal{S}}{\partial a_{\alpha\beta}}\, \Delta a_{\alpha\beta} + \frac{\partial \hat{W}_\mathcal{S}}{\partial \lambda_3}\, \Delta \lambda_3 \tag{152}$$

in the case of isotropy, allows us to identify constitutive relations (56) and (59).

B Proof of Eq. (143)

To prove Eq. (143), one can first show that

$$\boldsymbol{x}\cdot\left(\boldsymbol{n}\otimes\boldsymbol{a}^{\alpha}-\boldsymbol{a}^{\alpha}\otimes\boldsymbol{n}\right)\boldsymbol{w}_{,\alpha}=\boldsymbol{x}\cdot\left(\left(\boldsymbol{n}\otimes\boldsymbol{a}^{\alpha}-\boldsymbol{a}^{\alpha}\otimes\boldsymbol{n}\right)\boldsymbol{w}\right)_{;\alpha}\,. \tag{153}$$

Denoting the term in the outer parenthesis by $\boldsymbol{c}^{\alpha}$, one can now show that

$$\boldsymbol{x}\cdot\boldsymbol{c}^{\alpha}_{;\alpha}=2\,\boldsymbol{w}\cdot\boldsymbol{n}+\left(\boldsymbol{x}\cdot\boldsymbol{c}^{\alpha}\right)_{;\alpha}\,, \tag{154}$$

and then employ the surface divergence theorem to get

$$\int_{\mathcal{S}}\boldsymbol{x}\cdot\boldsymbol{c}^{\alpha}_{;\alpha}\,\mathrm{d}a=2\int_{\mathcal{S}}\boldsymbol{w}\cdot\boldsymbol{n}\,\mathrm{d}a+\int_{\partial\mathcal{S}}\boldsymbol{x}\cdot\boldsymbol{c}^{\alpha}\,m_{\alpha}\,\mathrm{d}s\,, \tag{155}$$

where m_{α} are the components of the boundary normal. So if $\mathcal{S}$ is closed, or if $\boldsymbol{w}=\boldsymbol{0}$ on $\partial\mathcal{S}$, one obtains (143) for $\boldsymbol{w}=\Delta\boldsymbol{x}$.

Acknowledgements

The author is grateful to the German Research Foundation (DFG) for supporting this research under projects SA1822/3-2, SA1822/5-1 and GSC 111. The author also thanks Callum J. Corbett for his help with the example in Sec. 5.

References

[1] Steigmann DJ. On the relationship between the Cosserat and Kirchhoff-Love theories of elastic shells. *Math. Mech. Solids* 1999; **4**:275–288.

[2] Steigmann DJ. Fluid films with curvature elasticity. *Arch. Rat. Mech. Anal.* 1999; **150**:127–152.

[3] Laursen TA. *Computational Contact and Impact Mechanics: Fundamentals of modeling interfacial phenomena in nonlinear finite element analysis*. Springer, 2002.

[4] Wriggers P. *Computational Contact Mechanics*. 2nd edn., Springer, 2006.

[5] Baesu E, Rudd RE, Belak J, McElfresh M. Continuum modeling of cell membranes. *Int. J. Non-lin. Mech.* 2004; **39**:369–377.

[6] Agrawal A. Mechanics of membrane-membrane adhesion. *Math, Mech. Solids* 2011; **16**(8):872–886.

[7] Sauer RA, Duong TX, Corbett CJ. A computational formulation for constrained solid and liquid membranes considering isogeometric finite elements. *Comput. Methods Appl. Mech. Engrg.* 2014; **271**:48–68.

[8] Chadwick P. *Continuum Mechanics: Concise Theory and Problems*. Dover, 1976.

[9] Andrade JD, King RN, Gregonis DE, Coleman DL. Surface characterization of poly(hydroxyethyl methacylate) and related polymers: I. Contact angle methods in water. *J. Polymer Science: Polymer Symposium* 1979; **66**(1):313–336.

[10] Lester GR. Contact angles of liquids at deformable solid surfaces. *J. Colloid Science* 1961; **16**:314–326.

[11] Lubarda VA. Mechanics of a liquid drop deposited on a solid substrate. *Soft Matter* 2012; **8**:10 288–10 297.

[12] Madasu S, Cairncross RA. Effect of substrate flexibility on dynamic wetting: a finite element model. *Comp. Meth. Appl. Mech. Engrg.* 2003; **192**:2671–2702.

[13] Madasu S, Cairncross RA. Static wetting on flexible substrates: a finite element formulation. *Int. J. Numer. Meth. Fluids* 2004; **45**:301–319.

[14] Léonforte F, Müller M. Statics of polymer droplets on deformable surfaces. *J. Chem. Phys.* 2011; **135**:214 703.

[15] Yu Y. Substrate elastic deformation due to vertical component of liquid-vapor interfacial tension. *Appl. Math. Mech. – Engl. Ed.* 2012; **33**(9):1095–1114.

[16] Pericet-Cámara R, Best A, Butt HJ, Bonaccurso E. Effect of capillary pressure and surface tension on the deformation of elastic surfaces by sessile liquid microdrops: An experimental investigation. *Langmuir* 2008; **24**:10 565–10 568.

[17] Steigmann DJ, Li D. Energy-minimizing states of capillary systems with bulk, surface and line phases. *IMA J. Appl. Math.* 1995; **55**(1):1–17.

[18] Sauer RA. Stabilized finite element formulations for liquid membranes and their application to droplet contact. *Int. J. Numer. Meth. Fluids* 2014; **75**(7):519–545.

[19] Johnson KL. *Contact Mechanics*. Cambridge University Press, 1985.

[20] Wriggers P. *Nonlinear Finite Element Methods*. Springer, 2008.

[21] Sauer RA. Enriched contact finite elements for stable peeling computations. *Int. J. Numer. Meth. Engrg.* 2011; **87**:593–616.